EPSC2017

SB6 abstracts

EPSC Abstracts
Vol. 11, EPSC2017-96, 2017
European Planetary Science Congress 2017
© Author(s) 2017

First results from stellar occultations in the "GAIA era"

G. Benedetti-Rossi (1,2,3) (gustavorossi@on.br), R. Vieira-Martins (1,2), B. Sicardy (4), the Rio Group, the "Lucky Star" Occultation Team, and the Granada Occultation Team
(1) Observatório Nacional/MCTIC, Brazil (2) Laboratório Interinstitucional de e-Astronomia (LineA), Brazil, (3) INCT do e-Universo/CNPq (4) Observatoire de Paris-Meudon, France

Abstract

Stellar occultation is a powerful technique to study distant solar system bodies. It allows high angular resolution of the occulting body from the analysis of a light curve acquired with high temporal resolution. In the past few years, this technique is showing impressive results such as the determination of Pluto's atmosphere with uncertainties comparable to the New Horizons probe[1], the discovery of rings around the Centaur object (10199) Chariklo[2], or the detection of a chasm on a Trans-Neptunian Object (2003 AZ84)[3], among others. After the first release of the GAIA catalog (in October/2016), stellar occultations predictions became much more accurate, which allowed us to observe several other stellar occultations. In this work we will present the improvement in orbit refinement for the outer solar system objects, some of the latest results obtained from stellar occultations, and the new chalenges to face.

1. Introduction

One big advantage of the stellar occultation technique is that it can be considered magnitude independent, in the sense that it is only necessary to detect light from the occulted star and not from the occulting body during the occultation. This allows both small and big telescopes to operate together and obtain impressive results[1,2,3]. On the other hand, stellar occultations present difficulties: they are transient events and require accurate predictions and can happen anywhere in the world, needing a huge collaboration network.

With the results from the GAIA space mission, stellar and bright TNO positions will be known with unprecedented accuracy, reaching values of the order of milliarcseconds. In other words, the prediction difficulty is overcome and the stellar occultation technique will now definitely be able to provide much more information about the sizes and shapes, presence of atmosphere, and also about the immediate neighborhoods of distant solar system bodies.

Stellar occultations by Pluto, (10199) Chariklo, (136108) Haumea, among many other objects are already in the list of the observed objects in the "GAIA era".

2. Summary and Conclusions

The GAIA mission (together with other surveys, such as the LSST) should provide accurate predictions of stellar occultations by tens of thousands of distant small solar system bodies in the next years. This will set a new era where a huge amount of unprecedent information will be acquired.

The participation of professional astronomers, laboratories, and the amateur community will be crucial to observe the predicted events. An easier method to coordinate observation campaigns, and the development of softwares capable of reducing the data more efficiently is needed

Stellar occultations observation campaigns will need to be selected according to a specific scientific prupose such as the probability to detect rings or archs around a body, the presence of atmosphere or even the detection of topographic features.

Acknowledgements

The authors want to thank the support of the CAPES (203.173/2016) and FAPERJ/PAPDRJ (E26/200.464/2015 – 227833) grants. Part of the research leading to these results has received funding from the European Research Council under the European Community's H2020 (2014-2020/ERC Grant Agreement no. 669416 "LUCKY STAR").

References

[1] Sicardy, B., Talbot, J.; Meza, E., et al.: Pluto's Atmosphere from the 2015 June 29 Ground-based Stellar Occultation at the Time of the New Horizons Flyby, The Astrophysical Journal Letters, Vol. Vol 819, Issue 2, L38, 8 pp. (2016).

[2] Braga-Ribas, F., Sicardy, B., Ortiz, J. L., et al.: A ring system detected around the Centaur (10199) Chariklo, Nature, Volume 508, Issue 7494, pp. 72-75 (2014).

[3] Dias-Oliveira, A., Sicardy, B., Ortiz, J. L., et al.: Study of the plutino object (208996) 2003 AZ 84 from stellar occultations: size, shape and topographic features, The Astronomical Journal, submitted (2017).

EPSC Abstracts
Vol. 11, EPSC2017-97, 2017
European Planetary Science Congress 2017
© Author(s) 2017

Physical characterization of Kuiper belt objects from stellar occultations and thermal measurements

P. Santos-Sanz and the SBNAF team.
Instituto de Astrofísica de Andalucía (IAA-CSIC), Glorieta de la Astronomía s/n, 18008-Granada, Spain (psantos@iaa.es)

Abstract

The knowledge of the physical and thermal properties (i.e. size, shape, density, albedo, thermal inertia, surface roughness) of the Kuiper belt objects (KBOs) is improving in the last times thanks to the record of stellar occultations produced by these objects [5] and by more sensitive observations and modeling of their thermal emissions [7,15]. Each of these techniques can take advantage of the other in order to improve the physical characterization of these icy bodies.

1. Introduction

Stellar occultations and thermal measurements of KBOs are complementary techniques to gain information on the physical and thermophysical properties of these objects. Both techniques are briefly described, and the state of the art of each one regarding the KBOs is presented.

2. Stellar occultations

Occultations by KBOs is a very direct and elegant technique to obtain sizes (with a few kilometers uncertainties), shapes and albedos of these bodies from the timing of a star disappearing and reappearing behind the object's limb [13]. In the last decade has been possible to predict and to observe stellar occultations by KBOs thanks to the best knowledge of their orbital elements and thanks to the improvement on the star positions from the available stellar catalogues. Around a dozen of KBOs have been characterized by stellar occultations up to date, including some of the largest (e.g. Eris [14], Makemake [8], Quaoar [2], 2007 UK_{126} [1], 2003 VS_2 [10], 2003 AZ_{84} [4], etc), and the ringed centaur Chariklo [3]. It is expected a significant increase in the number of stellar occultations by KBOs detected thanks to the use of the GAIA star catalogue to predict these events. This refinement will allow us the detection of stellar occultations by smaller KBOs than the detected up to date. GAIA DR1 catalogue is now available and improvements in predictions of stellar occultations are starting to be obvious, future GAIA realeases will improve the situation even more.

3. Thermal data

Radiometric technique provides diameters and albedos of KBOs from measures of their thermal emission. A thermal or thermophysical model applied to the thermal measurements, together with the knowledge of the absolute magnitude, allow us to obtain diameters and albedos, but with larger uncertainties (~10% in diameters and ~20% in albedos) than those obtained from stellar occultations. Thermal properties, like thermal inertia or surface roughness, can also be derived from thermophysical modeling. The maximum of the thermal emission for the KBOs is in the 70-160 μm range, these wavelengths are only reachable from space-based telescopes like Spitzer or Herschel. Spitzer has detected the thermal emission of a few dozens of KBOs [15] and Herschel Space observatory, within its key program "TNOs are Cool", has increased the number to ~140 objects (see [6,7,9] and references therein). For all these objects equivalent diameters, albedos and thermal properties have been derived.

4. Summary and Conclusions

Stellar occultations by KBOs provide very precise diameters and albedos while the radiometric technique is less accurate but allows accessing to a larger number of objects. There is a clear synergy between both techniques and it is possible to put both together in order to obtain a better physical and thermal characterization of these bodies [11,12]. It is also possible to improve the physical knowledge adding results obtained by other techniques like rotational light curves, photometry, spectra, etc, deriving a very complete physical portrait for

selected objects: this is the main goal of the European Union's funded project known as "Small Bodies Near and Far" (SBNAF). A sample of small bodies, including some of the most relevant KBOs, is being characterized within this project using a multi-technique approach.

Acknowledgements

This research has received funding from the European Union's Horizon 2020 Research and Innovation Programme, under Grant Agreement no 687378 and from the Spanish grant AYA-2014-56637-C2-1-P and the Proyecto de Excelencia de la Junta de Andalucía J.A. 2012-FQM1776.

References

[1] Benedetti-Rossi et al. AJ, 152, 156, 2016.

[2] Braga-Ribas et al. ApJ, 773, 26, 2013.

[3] Braga-Ribas et al. Nature, 508, 72, 2014.

[4] Dias-Oliveira et al. submitted to ApJ, 2016.

[5] Elliot et al. Nature, 465, 897, 2010.

[6] Lellouch et al. A&A, 557, A60, 2013.

[7] Müller et al. EM&P, 105, 209, 2009.

[8] Ortiz et al. Nature, 491, 566, 2012.

[9] Santos-Sanz et al. A&A, 541, A92, 2012.

[10] Santos-Sanz et al. ACM2017, Poster2.e.15, 2017.

[11] Santos-Sanz et al. A&A, in press, 2017.

[12] Schindler et al. A&A, 600, A12, 2016.

[13] Sicardy et al. Nature, 439, 52, 2006.

[14] Sicardy et al. Nature, 478, 493, 2011.

[15] Stansberry et al. The Solar System Beyond Neptune, 161, 2008.

EPSC Abstracts
Vol. 11, EPSC2017-140, 2017
European Planetary Science Congress 2017
© Author(s) 2017

Results from the New Horizons encounter with Pluto

C. B. Olkin (1), S. A. Stern (1), J. R. Spencer (1), H. A. Weaver (2), L. A. Young (1), K. Ennico (3) and the New Horizons Team

(1) Southwest Research Institute, Colorado, USA, (2) Johns Hopkins University Applied Physics Laboratory, Maryland, USA (3) NASA Ames Research Center, California, USA (colkin@boulder.swri.edu)

Abstract

In July 2015, the New Horizons spacecraft flew through the Pluto system providing high spatial resolution panchromatic and color visible light imaging, near-infrared composition mapping spectroscopy, UV airglow measurements, UV solar and radio uplink occultations for atmospheric sounding, and in situ plasma and dust measurements that have transformed our understanding of Pluto and its moons [1]. Results from the science investigations focusing on geology, surface composition and atmospheric studies of Pluto and its largest satellite Charon will be presented. We also describe the New Horizons extended mission.

1. Geology and Size

Highlights from the geology investigation of Pluto include the discovery of a unexpected diversity of geomorpholgies across the surface, the discovery of a deep basin (informally known as Sputnik Planitia) containing glacial ices undergoing mobile-lid convection [2] (Figure 1), evidence of glacial flow from topographic highs into the lower elevation basin, and a great diversity of surface ages ranging from the ancient (~4 Ga) age of the dark region dominating Pluto's equator to the relatively young (<10 Ma) age of the glacial ices. Pluto's radius was determined to be 1188 km [3], firmly establishing it as the largest body in the Kuiper Belt.

On Pluto's largest satellite, Charon, a large tectonic belt runs across its encounter hemisphere from northeast to southwest. There is significant vertical relief across Charon with more than 20 km variation in topography seen on Charon's limb and in stereo imaging [4].

The crater densities on Nix and Hydra, the larger of Pluto's four small moons, suggest ancient surface ages (~4 Ga), which is puzzling considering their high geometric albedos (~55% for Nix and ~80% for Hydra) and the various processes that would darken those surfaces over time [5].

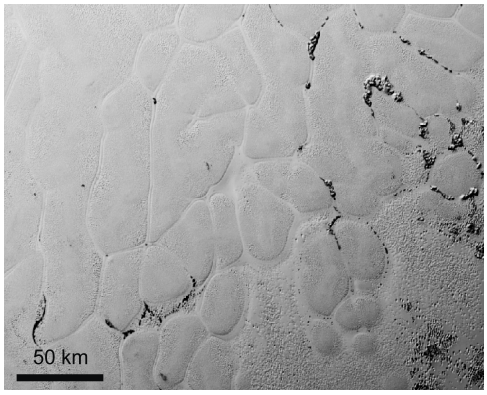

Figure 1: The glacial ices of Sputnik Planitia. The cellular pattern is a surface expression of mobile lid convection. The boundaries of the cells are troughs. Despite it's size of ~900,000 km^2, there are no identified craters across Sputnik Planitia.

2. Surface Composition

Using New Horizons imaging spectroscopy from 1-2.5 microns, we have created composition maps of volatile ices (N_2, CH_4, CO), non-volatile ices (H_2O), and tholins across the close approach hemisphere at spatial scales of kilometers. New Horizons obtained strong evidence for a water ice crust topped by a relatively thin veneer of volatiles. It was also found that Pluto's surface composition has patterns that depend on latitude. Pluto's equatorial region is dominated by non-volatile red material consistent with tholins, while the north pole is currently predominantly CH_4 ice. This can be explained by Pluto's seasonal insolation patterns.

Charon's surface spectra are dominated by absorptions from water ice, but multiple sites show absorption from a band centered near 2.21 microns,

which is probably associated with an NH_3-bearing molecule. The north pole of Charon is dark and red which, has been explained by atmospheric molecules escaping Pluto, intercepting Charon, becoming cold trapped at Charon's pole, then undergoing photolysis over Charon's ~100 year winter to form a layer of tholin-like material [6].

The near-IR spectra of Nix and Hydra are dominated by crystalline water ice absorption [7], consistent with their high geometric albedos and their formation from the ice-rich debris created during the collision that formed the Pluto-Charon system. The near-IR spectra of Nix and Hydra also show absorptions near 2.21 microns, presumably due to an NH_3-bearing species.

3. Atmospheres

The New Horizons investigation of Pluto's atmosphere [8] determined the temperature and pressure profiles in the atmosphere, the composition of the atmosphere as a function of altitude, the base surface pressure, the atmospheric escape rate, and the extensive nature of atmospheric haze on Pluto (see Figure 2). The escape rate was surprisingly small due to much lower than expected temperatures in the upper atmosphere. As a result the pressure balance with the solar wind was within ~6 times the radius of Pluto, much closer to Pluto than expected [9].

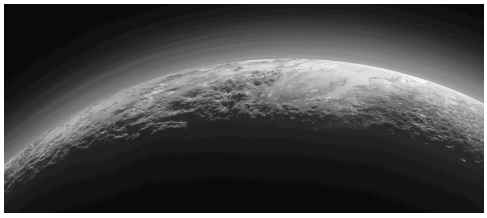

Figure 2: This image was taken by New Horizons just 15 minutes after closest approach. The highly forward scattering haze particles in Pluto's atmosphere are seen in the image. Layers of haze extend more than 200 km above Pluto's surface.

4. Extended Mission

New Horizons began a five year long extended mission to study the Kuiper Belt (KB) in October 2016. The goals of this mission are to study the dust, plasma and gas environment in the KB out to 50 AU, to observe numerous Kuiper Belt Objects (KBOs) and Centaurs at phase angles and resolutions unobtainable from Earth, and to conduct a close flyby of the KBO 2014 MU_{69}.

2014 MU_{69} is a member of the cold classical family of Kuiper belt objects, whose low orbital inclinations and low eccentricities suggest they are among the most primordial objects in the solar system. The flyby of 2014 MU_{69} will occur on January 1, 2019. Encounter objectives include high-resolution imaging, compositional mapping, stereo imaging, satellite and ring searches, coma searches, and more.

Acknowledgements

We thank NASA for funding the New Horizons project and this talk.

References

[1] Stern, S. A. et al.: The Pluto system: Initial results from its exploration by New Horizons, Science, Vol. 350, aad1815, 2015.

[2] McKinnon, W. B. et al.: Convection in a volatile nitrogen-ice-rich layer drives Pluto's geological vigour, Nature, Vol. 534, p. 82-85, 2016.

[3] Nimmo, F. et al.: Mean radius and shape of Pluto and Charon from New Horizons images, Vol. 287, p. 12-29, 2017.

[4] Moore, J. M. et al.: The geology of Pluto and Charon through the eyes of New Horizons, Science, Vol. 351, p. 1284-1293, 2016.

[5] Weaver, H. A. et al.: The small satellites of Pluto as observed by New Horizons, Science, Vol. 351, p. 1281, 2016.

[6] Grundy, W. et al.: The formation of Charon's red poles from seasonally cold-trapped volatiles, Nature, Vol. 539, p. 65-68, 2016.

[7] Cook, J. C. et al.: Composition of Pluto's Small Satellites: Analysis of New Horizons Spectral Images, LPSC, 2478, 2017.

[8] Gladstone, G. R. et al.: The atmosphere of Pluto as observed by New Horizons, Science, Vol. 351, p. 1280, 2016.

[9] Bagenal, F. et al.: Pluto's interaction with its space environment: Solar wind, energetic particles, and dust, Science, Vol. 351, p. 1282, 2016.

EPSC Abstracts
Vol. 11, EPSC2017-179, 2017
European Planetary Science Congress 2017
© Author(s) 2017

Serendipitous occultations by kilometer size Kuiper Belt with MIOSOTYS

A. Doressoundiram (1), C-Y. Liu (1), L. Maquet (1), F. Roques (1) and the MIOSOTYS team.

(1)LESIA, Observatoire de Paris, PSL Research University, CNRS, Univ. Paris Diderot, Sorbonne Paris Cité, UPMC Univ., Paris 06, Sorbonne Universités, 5 Place J. Janssen, Meudon Pricipal Cedex 92195, France (alain.doressoundiram@obspm.fr), (2).

Abstract

MIOSOTYS (Multi-object Instrument for Occultations in the SOlar system and TransitorY Systems) is a multi-fiber positioner coupled with a fast photometry camera. This is a visitor instrument mounted on the 193 cm telescope at the Observatoire de Haute-Provence, France and on the 123 cm telescope at the Calar Alto Observatory, Spain. Our immediate goal is to characterize the spatial distribution and extension of the Kuiper Belt, and the physical size distribution of TNOs. We present the observation campaigns during 2010-2013, objectives and observing strategy. We report the detection of potential candidates for occultation events of TNOs. We will discuss more specifically the method used to process the data and the modelling of diffraction patterns. We, finally present the results obtained concerning the distribution of sub-kilometer TNOs in the Kuiper Belt.

1. Introduction

As the Kuiper belt is located far from the sun, it is difficult to observe the small objects that are composing it. To understand how the Kuiper belt was formed, we need to study the size distribution of its objects. We have to be able to detect sub-kilometric objects. This is possible only by random stellar occultations. In order to perform those observations, we have an instrument called MIOSOTYS.

2. The instrument

MIOSOTYS consists of three parts : 30 fibre positioning arms (MEFOS) fixed on a platform, an Acquisition and Guiding Image System (AGIS) above the arm platform, and a CCD camera (ProEM CCD). It has been mounted as a visitor instrument on the 1.93-m telescope at Observatoire de Haute-Provence (OHP) in France since February 2010, and on the 1.23-m telescope at Calar Alto (CAHA) in Spain since November 2012.

The instrument has been upgraded from a past instrument, MEFOS (Meudon ESO Fibre Optical System, [1]). MIOSOTYS is a multi-fiber positioner coupled with a fast photometry camera. It is an arm positioner using 29 arms in a 26 arc-minute field. Each arm is equipped with an individual viewing system for accurate setting and carries one individual fiber that intercept 13" arcsec on the sky. All the 29 fibers are aligned on a CCD for fast photometry acquisition.

3. Observation and data analysis

Observations have been obtained during MIOSOTYS campaigns at OHP in 2010-2013 and at Calar-Alto afterwards at an acquisition rate of 20 Hz and with total median SNR of 25 (median SNR for OHP : 16 ; median SNR for Calar Alto : 34). Photometry has been obtained in a standard manner and lightcurve information has been extracted from the data. A total of 85

nights, that is about 9840 star-hours has been investigated for occultation events.

The search for outliers events is based on the detection of any data point deviant from the mean. A small size window is used in a middle of a large window used for computing mean and standard deviation in the stellar flux.

4. Modelling and fitting

The model : We consider that we are in the Fraunhofer diffraction regime [2]. The stellar flux is diffracted and smoothed on the observed bandwidth, on the stellar disc and on the integration step. The simulated pattern depends on several parameters (size and distance of the TNO, size of the star…).

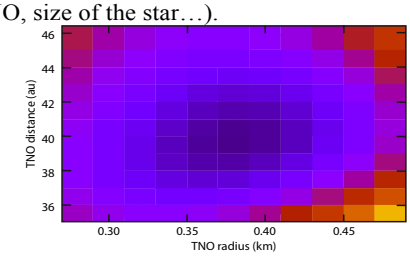

Figure 1 : (Left) X^2 map in relation with the radius and the distance of the TNO (violet : good fit, yellow : bad fit) (Right) Observation versus model (radius : 0.38 km ; TNO distance : 41 au)

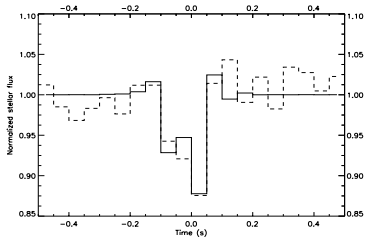

Figure 2 : Observation versus model (radius : 0.38 km ; TNO distance : 41 au)

The fit : We simulate several patterns with different sets of parameter values (the radius of the TNO varies between 0 and 1 km and its distance between 30 and 60 AU). Then, we compare the observation and the simulation by calculating the X^2. We search the set of values that minimize the X^2 . Below is an example of the procedure for one event.

5. Conclusions

Results of the fit and validation critrerion :

The algorithm detected 42 . On the 42 POEs, we found solutions for 7 of them in the following range :

- for the distance to the Sun : from 30 to 70 au

- for the radius of the TNO : from 0.01 to 1 km.

According to the validation criterion, only one of the 7 POEs with a solution can be considered as a real event (see Figure 6 ; distance : 41 ua and radius 380m).

Density in the sky plane :

Thanks to this detection, it is possible to deduce an estimation of the density of TNOs with a radius larger than 380m (see Figure 7 and see Liu et al. 2015 for the computation of the density). The value of this estimation is 6.40 $x10^7 deg^{-2}$. As we just obtain one positive POE, this value has to be considered as an upper limit. As we can on Figure 7, our result is consistent with the other determination.

References and Ackknowledgement

[1] P. Felenbok, J. Guérin, A. Fernandez, V. Cayatte, C. Balkowski,R. C. Kraan-Korteweg. 1997. The Performance of MEFOS, the ESO Multi-Object Fibre Spectrograph. Exper. Astron. 7 65-85. [2] F. Roques and M. Moncuquet. 2000. , Icarus, 147, 530 [3] C.-Y. Liu, A. Doressoundiram, F. Roques, H.-K. Chang, L. Maquet, M. Auvergne. 2015. MNRAS, 446, 932.

We acknowledge support from the European Research Council under the European Community's H2020 (2014-2020/ERC Grant Agreement 669416 "LUCKY STAR")

EPSC Abstracts
Vol. 11, EPSC2017-213, 2017
European Planetary Science Congress 2017
© Author(s) 2017

K2 and Herschel/PACS light curve of the Centaur 2060 Chiron

G. Marton (1), C. Kiss (1), T. G. Müller (2), E. Lellouch (3), A. Pál (1) and L. Molnár (1)
(1) Konkoly Observatory, Research Centre for Astronomy and Earth Sciences, Hungarian Academy of Sciences, Konkoly Thege 15-17, H-1121 Budapest, Hungary, marton.gabor@csfk.mta.hu, (2) Max-Planck-Institut für extraterrestrische Physik, Postfach 1312, Giessenbachstr., D-85741 Garching, Germany, (3) LESIA, Observatoire de Paris, PSL Research University, CNRS, Sorbonne Universités, UPMC Univ. Paris 06, Univ. Paris Diderot, Sorbonne Paris Cité, 5 place Jules Janssen, 92195, Meudon, France

Abstract

Recently 2060 Chiron was identified to harbor a ring system (Ortiz et al. 2015) similar to the other Centaur 10199 Chariklo (Braga-Ribas et al. 2014).

We observed 2060 Chiron in the visible range in Campaign 12 of the Kepler/K2 mission, that lasted from Dec 15 2016 to March 4 2017. We obtained the thermal light curve with the PACS photometer camera of the Herschel Space Observatory as a "Must Do Observation", taken at 70 and 160 μm on 25 December, 2012.

The presence of the ring affects the rotational light curve both in the visible range and in the thermal infrared. With our new observations we can disentangle the contribution of the main body and the ring material.

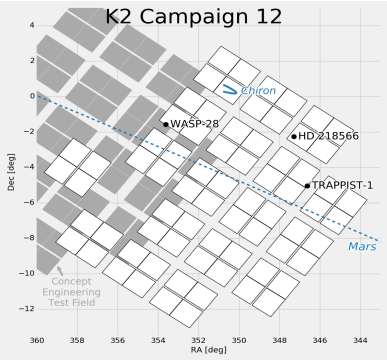

Figure 1: Visibility of 2060 Chiron in the Kepler/K2 Campaign 12.

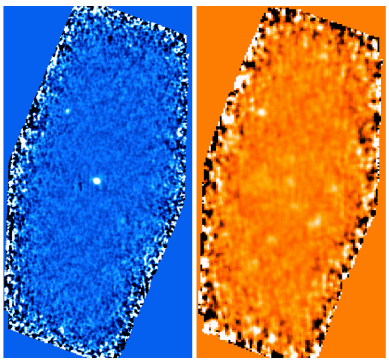

Figure 2: Chiron as seen by the Herschel/PACS in the blue (70 μm) and red (160 μm) bands.

Acknowledgements

Small Bodies Near And Far is a science project funded by European Commission in HORIZON 2020 Framework Programme for Research and Innovation under Grant agreement No 687378.

References

[1] Ortiz, J. L.; Duffard, R.; Pinilla-Alonso, N. et al. 2015, A&A, 576A, 18

[2] Braga-Ribas, F.; Sicardy, B.; Ortiz, J. L. et al. 2015, Nature, 508, 72

EPSC Abstracts
Vol. 11, EPSC2017-225, 2017
European Planetary Science Congress 2017
© Author(s) 2017

Formation of trans-Neptunian satellite systems at the stage of rarefied condensations

S. I. Ipatov (1,2)
(1) Vernadsky Institute of Geochemistry and Analytical Chemistry of Russian Academy of Sciences, Moscow, Russia (siipatov@hotmail.com, http://siipatov.webnode.ru/); (2) Space Research Institute of Russian Academy of Sciences, Moscow, Russia

Abstract

Formation of satellite systems of trans-Neptunian objects at the stage of rarefied condensations (consisted of dust and objects with diameter less than 1 m) is studied. It is considered that the main fraction of the angular momentum of a parental condensation needed for such formation was acquired at a collision of two condensations. Orbits of secondaries around primaries in discovered trans-Neptunian binary objects can be explained with the use of the considered model of formation of satellite systems.

1. Introduction

It is considered by many scientists that solid planetesimals were formed by contraction of rarefied condensations, which consisted of dust and/or boulders with diameter up to 1 m [1]. Ipatov [2] and Nesvorny et al. [3] supposed that trans-Neptunian binaries have been formed as a result of contraction of some such rarefied condensations. The angular momenta acquired at collisions of condensations that were moving in circular heliocentric orbits could have the same values as the angular momenta of discovered trans-Neptunian and asteroid binaries with masses equal to the sum of masses of two collided condensations [2].

2. Angular momenta of condensations needed for formation of binaries

The angular momenta used by Nesvorny et al. [3] as initial data in their calculations of contraction of condensations leading to formation of binaries could be obtained at collisions of two condensations that were moving before collisions in circular heliocentric orbits [4-5]. Initial angular momenta of condensations [6] were not enough for formation of binaries [5]. The typical angular momentum obtained at a collision of two identical uniform condensations can be greater by an order of magnitude than the sum of initial angular momenta of the collided condensations. If radii of two uniform condensations decreased before their collision from their initial radii by a factor of more than 3, then the angular momentum due to a typical collision is smaller than that due to initial rotation of condensations. For condensations more dense to their centers this factor is greater. At the ratio of radii of collided uniform condensations of different masses greater than 3, the role of initial rotation in the angular momentum of the formed condensation is greater than that of the collision. For the considered model at which the parental condensation that formed at a collision contracted to form a solid binary system, more chances to form a binary were for greater distances from the Sun.

The parental condensation with radius close to its Hill radius that grew by accumulation of small objects could get the angular momentum at which a satellite system of a trans-Neptunian object could form. However, in this case the angular momentum of all satellite systems (e.g., binaries) would be positive. Actually about 40% of observed trans-Neptunian binaries have negative angular momentum. Depending on heliocentric orbits of two colliding condensations, the angular momentum at their collision can be positive or negative. Therefore in most cases the greater fraction of the angular momentum of a parental condensation that contracted to form a trans-Neptunian binary was acquired at a collision of condensations, but not by accumulation of small objects. However, some fraction of the angular momentum of parental condensations could be delivered by small objects. I suppose that the fraction of condensations collided with other condensations during their contraction can be about the initial fraction of small bodies of diameter d>100 km with satellites (among all such small bodies), i.e., it can be about 0.45 in the trans-Neptunian belt. The

results presented in this section are discussed in details in [5].

3. Origin of orbits of secondaries in discovered trans-Neptunian binaries

Based on the data presented in http://www.johnstonsarchive.net/astro/astmoons/, I studied [7-8] prograde and retrograde rotation of discovered trans-Neptunian binaries, the inclinations of orbits of secondaries at different ratios of diameters of the secondary to the primary, the inclinations of orbits of secondaries at different orbital elements of heliocentric orbits of binaries, the separation distances at different heliocentric orbits, the orbits of binaries at different separation distances. It was shown that all these dependences can be explained for our model of formation of binaries at the stage of rarefied condensations. A few of such dependencies are discussed below.

The fraction of trans-Neptunian objects with inclinations i_s of orbits of secondaries (or of orbits of the largest satellites) greater than 90^o is about 0.4. For all four satellite systems with eccentricity of the heliocentric orbit e>0.3, i_s<90^o. The values of i_s are in a wide range, almost from 0 to 180^o. The absence of binaries with i_s>130^o at the ratio of diameters of the secondary to the primary d_s/d_p<0.7 may be caused by that the contribution of initial positive angular momentum of the collided condensations to the final angular momentum of the parental condensation was greater at d_s/d_p<0.7 than at d_s/d_p>0.7. It could be caused by that masses of collided condensations differed more at smaller d_s/d_p.

For e>0.3 the ratio a_s/r_H of the separation a_s between the primary and the secondary to the Hill radius r_H of the binary was smaller than 0.024, while a_s/r_H can exceed 0.225 at e<0.3. Note that the trans-Neptunian objects with e>0.3 could form in the feeding zone of the giant planets (see, e.g., [9]), i.e., closer to the Sun than the objects with e<0.3. Maximum values of a_s/r_H (and also of a_s) are greater for greater semi-major axis a of a heliocentric orbit of an object at 38<a<46 AU. In our opinion, for smaller distances a from the Sun, the mean sizes of collided condensations could be smaller, and so the mean values of a_s for the formed binaries could be smaller. The smaller sizes of the collided condensations at smaller distances from the Sun could be due to their smaller Hill radii (which are proportional to a) at the collisions and, may be, also due to faster contraction of condensations.

For a_s/r_H<0.008, except one object, the values of i_s are between 60^o and 105^o, i.e., are in some vicinity of 90^o. Probably, the origin of such i_s was caused by that for smaller sizes of collided condensations (that produce binaries with smaller a_s/r_H), the ratio of their sizes to the height of the disk where condensations moved was smaller, and collided condensations often moved one above another, but not in almost the same plane as in the case when the sizes of condensations were about the height.

Acknowledgements

The work was supported in part by the grant of Russian Foundation for Basic Research № 17-02-00507 A and by the Program of the Fundamental Studies of the Presidium of the Russian Academy of Sciences N 9.

References

[1] Johansen, A., Mac Low, M.-M., Lacerda, P., Bizzarro M.: Science Advances, Vol. 1, N 3, id. 1500109, 2015 (http://arxiv.org/abs/1503.07347).

[2] Ipatov, S.I.: Mon. Not. R. Astron. Soc., Vol. 403, pp. 405-414, 2010.

[3] Nesvorny, D., Youdin, A.N., Richardson, D.C.: Astron. J., Vol. 140, pp. 785-793, 2010.

[4] Ipatov, S.I.: Proc. IAU Symp. No. 293 "Formation, detection, and characterization of extrasolar habitable planets", pp. 285-288, 2014 (http://arxiv.org/abs/1412.8445).

[5] Ipatov, S.I.: Solar System Research, Vol. 51, N 4, in press, 2017.

[6] Safronov, V.S.: Evolution of the protoplanetary cloud and formation of the Earth and the planets. NASA TTF-677, 212 p., 1972.

[7] Ipatov, S.I. Abstracts of 46th LPSC, #1512, 2015.

[8] Ipatov, S.I.: Solar System Research, Vol. 51, N 5, in press, 2017.

[9] Ipatov, S.I.: Earth, Moon, & Planets, Vol. 39, pp. 101-128, 1987.

EPSC Abstracts
Vol. 11, EPSC2017-237-1, 2017
European Planetary Science Congress 2017
© Author(s) 2017

Search for sub-kilometre trans-Neptunian objects using all CoRoT AN1 Light-curves

C.-Y. Liu (1,2), A. Doressoundiram (1), F. Roques (1), H.-K. Chang (2), S. Chaintreuil (1)
(1) LESIA, Observatoire de Paris, Meudon, France, (2) Institute of Astronomy, National Tsing Hua University, Hsinchu, Taiwan (chihyuan.liu@obspm.fr)

Abstract

We present here the analysing results of using all CoRoT (Convection Rotation and Planetary Transits) asteroseismological N1 light-curves with the serendipitous stellar occultation method. We will report our combining result in this meeting, and also the comparisons with other surveys.

1. Introduction

Trans-Neptunian Objects (TNOs) are the witnesses of the formation of the planets during the dynamical and collisional period of our solar system. The population characteristics of sub-kilometer sized TNOs may carry some important clues for the origin of the planets. However, the knowledge of them is far from enough, particularly for those smaller ones, due to very few detections. Nowadays only TNOs larger than about 25 km can be directly observed. For the TNOs not able to be directly observed, searching for serendipitous stellar occultation events is a possible method. Currently, from the literature, only 15 Possible Occultartion Events (POEs) are reported from two serendipitous surveys: 2 POEs are found by Schlichting et al. using the observations taken by the Hubble Space Telescope's Fine Guidance Sensors [1], and the other 13 are found in our previous work using CoRoT data [2].

2. New CoRoT AN1 data sets

We analyzed the rest of CoRoT AN1 data which contains 188 lightcurves from 77 stars monitored within 16 observation runs, in total about 130.4k star-hours, in addition to the 144.4k star-hours we previously dealt with (See Table 1 for more details). Using deviation method [2], we got 12 new outliers. 10 of them might not be related to any instrumental effects after checking raw data by CoRoT team.

Table 1: Comparions of CoRoT data employed in our earlier and current works.

CoRoT AN1 Data	Liu2015	New
# 1-sec Bins	519869933	469411359
Exposure (star-hours)	144.4×10^3	130.4×10^3
# RunCodes	9	16
# AN1 light-curves	165	188
# Background Stars	79	77
# POEs/Outliers	13/20	10/12

3. Results and Conclusion

We got 23 POEs from analyzing total CoRoT asteroseismology observations which is about 274.8k star-hours. The minimal sizes of these possible occultors orbiting beyond Neptune are ranging from 0.4 to 1.5 km. The new combining result will help us to refine our earlier estimate of TNO size distribution as shown in Figure 1.

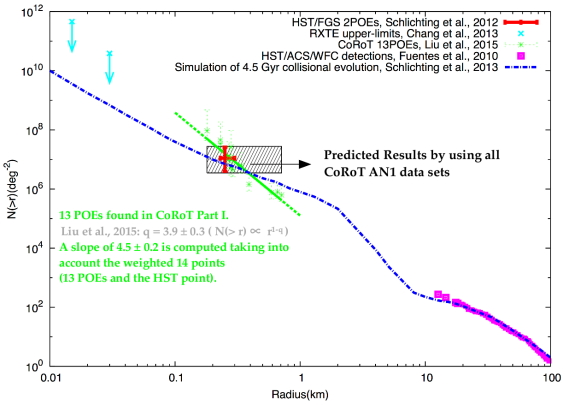

Figure 1: A possible result on size distribution of the sub-kilometre TNOs using all CoRoT AN1 data. Results, Upper-limits from other surveys and a possible modle are also plotted.

Acknowledgements

CoRoT space mission has been developed and is operated by the French Space agency CNES in collaboration with Austria, Belgium, Brazil, ESAs RSSd and Science Programs, Germany, and Spain. We acknowledge support from the European Research Council under the European Community's H2020 (2014-2020/ERC Grant Agreement 669416 "LUCKY STAR"). This work was also supported by the Programme National de Planétologie (PNP) and the Agence National pour la Recherche of France, and also by National Science Council of the Republic of China (Taiwan).

References

[1] Schlichting, H. E., Ofek, E. O., Sar, R. et al., 2012, ApJ, 761, 150

[2] Liu, C.-Y., Doressoundiram, A., Roques, F., Chang, H.-K., Maquet, L., Auvergne, M., 2015, MNRAS, 446, 932

EPSC Abstracts
Vol. 11, EPSC2017-321-2, 2017
European Planetary Science Congress 2017
© Author(s) 2017

The 2017 January 21st multi-chord stellar occultation by the dwarf planet Haumea. Preliminary results.

J. L. Ortiz (1), **P. Santos-Sanz** (1), B. Sicardy (2), F. Braga-Ribas (3,4), N. Morales (1), R. Duffard (1), U. Hopp (5,6), C. Ries (5), V. Nascimbeni (7,8), F. Marzari (9), V. Granata (7,8), A. Pál (10), C. Kiss (10), T. Pribulla (11), R. Komžík (11), K. Hornoch (12), P. Pravec (12), P. Bacci (13), M. Maestripieri (13), M. Bachini (14,15), F. Martinelli (15), G. Succi (15), F. Ciabattari (16), H. Mikuz (17), A. Carbognani (18), B. Gaehrken (19), S. Mottola (20), S. Hellmich (20), D. Berard (2), G. Benedetti-Rossi (3), F. Rommel (21), A. Campo Bagatin (22), S. Cikota (23), A. Cikota (24), J. Lecacheux (2), R. Vieira-Martins (3,25), J.I.B. Camargo (3,26), M. Assafin (27), F. Colas (25), R. Behrend (28), J. Desmars (25), E. Meza (2), R. Leiva (2,29), E. Fernández-Valenzuela (1), W. Beisker (30), A. R. Gomes-Junior (27), F. Roques (2), F. Vachier (25), T. G. Mueller (6), J. M. Madiedo (31), O. Unsalan (32), E. Sonbas (33), N. Karaman (33), O. Erece (34), D.T. Koseoglu (34), T. Ozisik (34), S. Kalkan (35), Y. Guney (36), M.S. Niaei (37), O. Satir (37), C. Yesilyaprak (37,38), C. Puskullu (39), A. Kabas (39), O. Demircan (39), V. Charmandaris (40), G. Leto (41), J. Ohlert (42), R. Szakáts (10), A. Takácsné Farkas (10), E. Varga-Verebélyi (10), G. Marton (10), A. Marciniak (43), P. Bartczak (43), T. Santana-Ros (43), M. Butkiewicz-Bąk (43), G. Dudziński (43), V. Alí-Lagoa (6), K. Gazeas (44), N. Paschalis (45), V. Tsamis (46), A Sanchez-Lavega (47), S. Pérez-Hoyos (47), R. Hueso (47), J. C. Guirado (48), V. Peris (48), R. Iglesias-Marzoa (49,50)

(1) Instituto de Astrofísica de Andalucía (CSIC), Granada, Spain, (2) LESIA/Observatoire de Paris, Université Pierre et Marie Curie, Université Paris-Diderot, Meudon, France, (3) Observatório Nacional/MCTI, Rio de Janeiro, Brazil, (4) Federal University of Technology-Paraná (UTFPR / DAFIS), Curitiba, Brazil, (5) Universitäts-Sternwarte München, München, Germany, (6) Max–Planck–Institut für extraterrestrische Physik (MPE), Garching, Germany, (7) Dipartimento di Fisica e Astronomia, 'G. Galilei', Università degli Studi di Padova, Padova, Italy, (8) INAF-Osservatorio Astronomico di Padova, Padova, Italy, (9) Department of Physics, University of Padova, Padova, Italy, (10) Konkoly Observatory of the Hungarian Academy of Sciences, Budapest, Hungary, (11) Astronomical Institute, Slovak Academy of Sciences, Tatranská Lomnica, Slovakia, (12) Astronomical Institute, Academy of Sciences of the Czech Republic, Ondřejov, Czech Republic, (13) Astronomical Observatory San Marcello Pistoiese CARA Project, Italy, (14) Osservatorio Astronomico di Tavolaia, Pisa, Italy, (15) Lajatico Astronomical Centre, Pisa, Italy, (16) Osservatorio Astronomico di Monte Agliale, Lucca, Italy, (17) Črni Vrh Observatory, Črni Vrh nad Idrijo, Slovenia, (18) Astronomical Observatory of the Autonomous Region of the Aosta Valley, (19) Volkssternwarte München, Germany, (20) German Aerospace Center (DLR), Institute of Planetary Research, Berlin, Germany, (21) Universidade Federal da Fronteira Sul, UFFS, Santa Catarina, Brazil, (22) Universidad de Alicante, Alicante, Spain, (23) Department of Applied Physics, Faculty of Electrical Engineering and Computing, University of Zagreb, Zagreb, Croatia, (24) European Southern Observatory, München, Germany, (25) IMCCE/Observatorie de Paris, Paris, France, (26) Laboratório Interinstitucional de e-Astronomia - LIneA, Rio de Janeiro, Brazil, (27) Observatório do Valongo/UFRJ, Rio de Janeiro, Brazil, (28) Observatoire de Genève, Sauverny, Switzerland, (29) Instituto de Astrofísica, Facultad de Física, Pontificia Universidad Católica de Chile, Santiago, Chile, (30) International Occultation Timing Association - European Section (IOTA-ES), Germany, (31) Departamento de Física Atómica, Molecular y Nuclear, Facultad de Física, Universidad de Sevilla, Sevilla, Spain / Facultad de Ciencias Experimentales, Universidad de Huelva, Huelva, Spain, (32) Ege University, Faculty of Science, Department of Physics, Izmir, Turkey, (33) University of Adiyaman, Department of Physics, Adiyaman, Turkey, (34) TUBITAK National Observatory (TUG), Akdeniz University Campus, Antalya, Turkey, (35) Ondokuz Mayis University Observatory, Space Research Center, Samsun, Turkey, (36) Atatürk University, Science Faculty, Department of Physics, Erzurum, Turkey, (37) Atatürk University, Astrophysics Research and Application Center (ATASAM), Erzurum, Turkey, (38) Atatürk University, Science Faculty, Department of Astronomy and Astrophysics, Erzurum, Turkey, (39) Canakkale Onsekiz Mart University, Astrophysics Research Center (ARC) and Ulupınar Observatory (UPO), Canakkale, Turkey, (40) Institute for Astronomy, Astrophysics, Space Applications & Remote Sensing, National Observatory of Athens, Athens, Greece / University of Crete, Department of Physics, Heraklion, Greece, (41) INAF-Catania Astrophysical Observatory, Sicilia, Italy, (42) Michael Adrian Observatorium, Astronomie Stiftung Trebur, Trebur, Germany / University of Applied Sciences, Technische Hochschule Mittelhessen, Friedberg, Germany, (43) Astronomical Observatory Institute, Faculty of Physics, A. Mickiewicz University, Poznań, Poland, (44) National and Kapodistrian University of Athens, Greece, (45) Nunki Observatory, (46) Elllinogermaniki Agogi Observatory, (47) Departamento de Física Aplicada I, Escuela de Ingeniería de Bilbao, Universidad del País Vasco UPV /EHU, Bilbao, Spain, (48) Observatorio Astronómico, Universidad de València, Valencia, Spain, (49) Centro de Estudios de Física del Cosmos de Aragón,Teruel, Spain, (50) Dpto de Astrofísica, Universidad de La Laguna, Tenerife, Spain

(ortiz@iaa.es)

Abstract

We will report exciting results from a multi-chord stellar occultation by dwarf planet Haumea on 2017 January 21st recorded with 12 telescopes at 10 observatories in Europe. This is the best occultation by a Trans-Neptunian Object ever published, in terms of the number of chords. Among the most interesting results, the 12 chords of the occultation allowed us to fit an ellipse for the limb of Haumea at the moment of occultation with kilometric accuracy. A new 3D shape for Haumea is derived from the occultation data combined with rotational light curve data. And also accurate density and albedo are determined for Haumea for the first time. Upper limits on the surface pressure of a N_2 or CH_4-dominated atmosphere are derived too.

1. Introduction

Haumea is a very exotic Trans-Neptunian Object (TNO) with unique characteristics [1,2,3,5] and is the only of the four objects currently classified as dwarf planets in the trans-neptunian region for which there aren't accurate determinations of their main physical properties (i.e. size, shape, albedo and density). For the other three dwarf planets, we have very precise determinations of these physical properties by means of stellar occultations and/or spacecraft visits [4,6,7].

Within our program to obtain physical properties of TNOs we predicted an occultation of the star URAT1 533-182543 (GaiaDR1 1233009038221203584) by the dwarf planet Haumea and arranged observations within the expected shadow path in Europe. The star is of similar brightness (R~15.7 mag) as Haumea, so medium to large telescopes were needed to record the occultation with sufficient signal to noise ratio.

2. Observations

Series of CCD images were obtained with different telescopes, and 12 of them recorded the disappearance and reappearance of the star. This is already a breakthrough because no stellar occultation by a TNO had ever been observed with so many chords. The telescopes that recorded positive observations were the following ones: the Wendelstein Observatory 2m telescope and the 0.4m telescope (Germany), the Skalnate Pleso Observatory 1.3m telescope (Slovakia), the Konkoly Observatory 1m telescope and the 0.6m telescope (Hungary), the Bavarian Public Observatory 0.81m telescope in Munich (Germany), the Ondrejov Observatory 0.65m telescope (Czech Republic), the Crni Vrh observatory 0.6m telescope (Slovenia), the S. Marcello Pistoiese observatory 0.6m telescope (Italy), the Lajatico Astronomical Centre 0.5m telescope (Italy) the Mount Agliale observatory 0.5m telescope (Italy) and the Asiago observatory, 1.8m telescope at Cima Ekar (Italy).

3. Main results

From the positive occultation observations we derived light curves which showed deep drops of different duration around the predicted occultation time. As these curves are abrupt at disappearance and reappearance of the star, Haumea must lack a global atmosphere of the type seen in Pluto. From the chords of the occultation produced by the main body we fitted an ellipse, which represents the instantaneous limb of Haumea at the moment of the occultation. This information, together with a very precise rotational light curve, allowed us to reconstruct the full 3D shape of this dwarf planet. We have found remarkable features that will be discussed in this conference.

Acknowledgements

Support by the Spanish grant AYA-2014-56637-C2-1-P and the Proyecto de Excelencia de la Junta de Andalucía J.A. 2012-FQM1776. Part of the research leading to these results has received funding from the European Union's Horizon 2020 Research and Innovation Programme, under Grant Agreement no 687378. Part of the research leading to these results has received funding from the European Research Council under the European Community's H2020 (2014-2020/ERC Grant Agreement no. 669416).

References

[1] Brown, M. E. et al. AJ. 632, L45-L48, 2005. [2] Brown, M. E. et al. Nature 446, 294-296, 2007. [3] Lockwood, A. C. et al. EM&P 111, 127-137, 2014. [4] Ortiz, J. L. et al. Nature 491, 566-569, 2012. [5] Rabinowitz, D. L.et al. AJ. 639, 1238-1251, 2006. [6] Sicardy, B. et al. Nature 478, 493-496, 2011. [7] Stern, S. A.et al. Science 350, aad1815, 2015.

EPSC Abstracts
Vol. 11, EPSC2017-330, 2017
European Planetary Science Congress 2017
© Author(s) 2017

Methanol ice on Kuiper Belt objects 2007 OR_{10} and Salacia: Implications for formation and dynamical evolution

B. J. Holler (1), L.A. Young (2), S.J. Bus (3), S. Protopapa (4)
(1) Space Telescope Science Institute, Baltimore, Maryland, USA, (2) Southwest Research Institute, Boulder, Colorado, USA, (3) Institute for Astronomy, Hilo, Hawaii, USA, (4) University of Maryland, College Park, Maryland, USA.
(bholler@stsci.edu / tel: +1-410-338-6404)

Abstract

Kuiper Belt Objects (KBOs) and Centaurs are effective tracers of Solar System formation and evolution. We present low-resolution, near-infrared spectra of the scattered disk object (225088) 2007 OR_{10} and the hot classical KBO (120347) Salacia obtained with IRTF/SpeX in Prism mode. We identify H_2O absorption features on both objects and an additional feature at 2.27 μm that we interpret as being due to methanol. The presence of methanol and H_2O can possibly explain the observed surface properties of 2007 OR_{10}, but it is more difficult to reconcile methanol on Salacia because of its neutral-colored surface.

1 Introduction

The properties of the Solar System's different minor body populations, such as the Centaurs and KBOs, provide valuable information on the formation and dynamical evolution of the entire Solar System. The orbital parameters and size of the population indicate which dynamical processes were important early in Solar System history while surface properties reveal the composition of different regions of the solar nebula. Surface properties include broadband colors and composition, which are linked. Two general varieties of surface are observed among the Centaurs and KBOs: low albedo/neutral color (dark/neutral) and high albedo/red color (bright/red) ([1], [2]). Theoretical work suggests these colors are the result of initial surface composition and are not altered during later periods of dynamical evolution: irradiation of H_2O and CO_2 on objects that formed closer to the Sun creates a dark/neutral surface while irradiation of CH_3OH (methanol) creates a bright/red surface [3]. Methanol was previously identified on the Centaur Pholus [4] and the KBO 2002 VE_{95} [5], two bright/red objects. However, dark/red and bright/neutral surfaces are also observed [1], albeit in lower numbers, that cannot be explained by the simple model of [3].

2 Observations

In this work we obtained near-infrared (0.7-2.5 μm) spectra of the large, faint KBOs (225088) 2007 OR_{10} and (120347) Salacia at NASA's Infrared Telescope Facility using the SpeX instrument in low-resolution (R$\sim$75) Prism mode. Observations of 2007 OR_{10} on October 15, 16 and November 3, 2015, and Salacia on November 2, 4, 2015, yielded 8.3 and 6.9 hours of time-on-target, respectively. 2007 OR_{10} is a scattered disk object currently $\sim$87 AU from the Sun and had a V magnitude of 22.0 at the time of the observations. It is a dark/red object [6] with an albedo of $0.089\pm^{0.031}_{0.009}$ [7]. Salacia is a hot classical KBO $\sim$45 AU from the Sun and had a V magnitude of 20.6 at the time of the observations. Salacia is a dark/neutral object with an albedo of 0.044$\pm$0.004 [8] and a B-R color of 1.067$\pm$0.115 [9].

3 Analysis

The KBO spectra were reduced with Spextool [10] and combined spectra were created for both objects (Figures 1 & 2). A model consisting of spectral slope and y-offset components and an H_2O ice spectrum was fit to each combined spectrum using a least-squares fitting algorithm. We also calculated the reduced χ^2 taking into account 3 free parameters.

4 Results & discussion

As seen in Figures 1 & 2, H_2O ice is present on both KBOs, at least in the amorphous phase since the spectral resolution and SNR are not adequate enough to

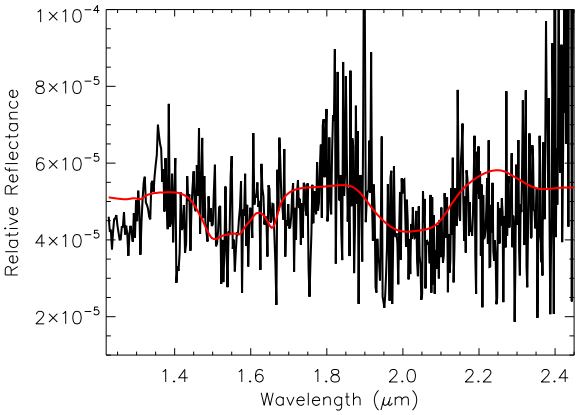

Figure 1: Near-infrared spectrum of scattered disk object (225088) 2007 OR_{10} from 1.4-2.45 μm. The data are in black with an H_2O model overplotted in red. $\chi^2_{\rm reduced}$=2.52

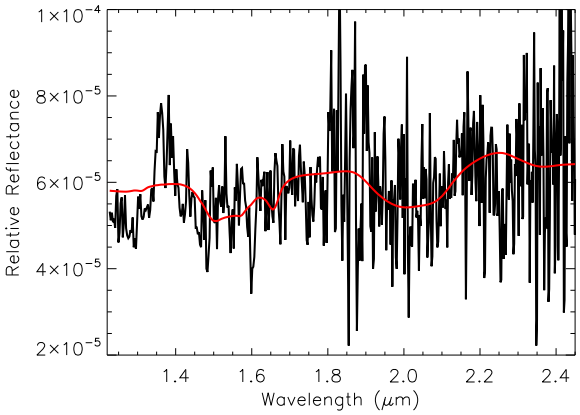

Figure 2: Near-infrared spectrum of hot classical KBO (120347) Salacia from 1.4-2.45 μm. The data are in black with an H_2O model overplotted in red. $\chi^2_{\rm reduced}$=1.79

make an identification of the 1.65 μm crystalline H_2O feature. Since $\chi^2_{\rm reduced}>1$, H_2O is not the only component. This is partially due to the bad fit at shorter wavelengths and the residual noise from the telluric correction between $\sim$1.8-1.9 μm, but is also due to the additional absorption feature observed near 2.27 μm that is not fit by the H_2O ice model. Based on previous work ([4], [5]), we interpret this feature as due to methanol and/or its irradiation products. The same feature was previously observed in the spectrum of Salacia but was not discussed [11].

The presence of methanol on the surfaces of 2007 OR_{10} (dark/red) and Salacia (dark/neutral) does not agree with the simple model of [3]. Methanol and its irradiation products, based on laboratory experiments, are expected to result in a bright/red surface. On 2007 OR_{10}, it is possible that irradiation of H_2O is responsible for the darker surface, but the dark/neutral surface of Salacia is harder to reconcile with the presence of methanol. Salacia may have formed in a transition region where the resulting color was not dominated by a single surface component, as expected for methanol and the bright/red KBOs. Some other species was likely present on the surface of Salacia early in Solar System history. Further laboratory work is needed to identify potential species that would result in surfaces like Salacia's. Additional spectral observations of dark/neutral KBOs are needed to quantify the number of Salacia-like objects.

References

[1] Lacerda, P., et al., 2014. ApJL, 793, L2.

[2] Tegler, S.C., et al., 2016. AJ 152, 210.

[3] Brown, M.E., et al., 2011. ApJL 739, L60.

[4] Cruikshank, D.P., et al., 1998. Icarus 135, 389-407.

[5] Barucci, M.A., et al., 2006. A&A 455, 725-730.

[6] Brown, M.E., et al., 2011. ApJL 738, L26.

[7] Pál, A., et al., 2016. AJ 151, 117.

[8] Fornasier, S., et al., 2013. A&A 555, A15.

[9] Hainaut, O.R., et al., 2012. A&A 546, A115.

[10] Cushing, M.C., et al., 2004. PASP 116, 362-376.

[11] Schaller, E.L., Brown, M.E., 2008. ApJ 684, L107-L109.

EPSC Abstracts
Vol. 11, EPSC2017-363, 2017
European Planetary Science Congress 2017
© Author(s) 2017

Spectroscopy of the dwarf planet Makemake

T. Hromakina (1, 2), D. Perna (2, 3), F. Merlin (2), S. Ieva (3), S. Fornasier (2), I. Belskaya (1) and E. Mazzotta Epifani (3)
(1) Institute of Astronomy, Kharkiv V.N. Karazin National University, Sumska Str. 35, Kharkiv 61022, Ukraine, (2) LESIA – Observatoire de Paris, PSL Research University, CNRS, Sorbonne Universités, UPMC Univ. Paris 06, Univ. Paris Diderot, Sorbonne Paris Cité, 5 place Jules Janssen, F-92195 Meudon, France, (3) INAF – Osservatorio Astronomico di Roma, Via Frascati 33, I-00078 Monte Porzio Catone (Roma), Italy

Abstract

Here we present new rotationally resolved visible and near-infrared spectra of the dwarf planet Makemake obtained in the time span 2006–2013. Our spectra show no variation within the errors, suggesting a very homogeneous surface, as well as no secular variations was discovered when comparing our data to that in the literature. The presence of methane diluted in nitrogen is evidenced by the shift of the observed absorption bands with respect to those of pure methane. Spectral modelling results suggest that the addition of methane irradiation products gives better fit to our data compared to that of pure methane ice.

1. Introduction

The spectrum of dwarf planet (136472) Makemake is dominated by the deep absorption bands of methane ice (associated with large grain sizes), that are slightly blue-shifted with respect to those of pure methane, suggesting the latter is the dominant material with a possible partial dilution in nitrogen (cf. [4] and references therein). Additionally, a polarimetric observation of Makemake suggests the presence of a thin low-porosity layer of hoarfrost [1]. Thermal observations of Makemake suggest the presence of a low-albedo spot on an overall high-albedo surface [2]. But the recent discovery of a Makemake's satellite [3] makes plausible to associate the dark material with the surface of the satellite. Noteworthy, the first rotationally resolved spectroscopy of Makemake [4] did not show a reliable variation and keeps Makemake's surface heterogeneity open to discussion.

2. Observations

A total of 12 visible (Figure 1) and 2 near-infrared

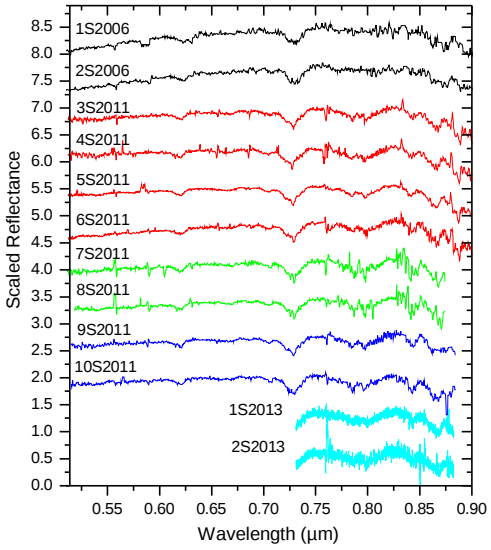

Figure 1: Visible reflectance spectra of Makemake obtained in 2006-2013.

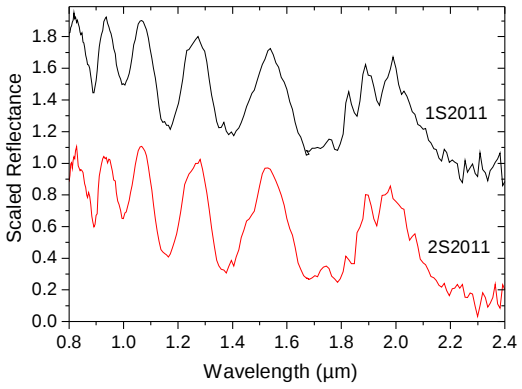

Figure 2: NIR reflectance spectra of Makemake obtained on 28/29 March 2011.

(NIR) (Figure 2) spectra were obtained in 2006–2013 during three observing runs (April 2006, March 2011 and January 2013). All observations were carried out at the 3.6-m TNG telescope (La Palma, Spain), using

the DOLORES instrument for visible observations and the NICS instrument for NIR observations. Data reduction has been performed following the standard procedure using the IRAF software package.

3. Data analysis

The majority of spectra were obtained during the second run in 2011, covering about 80 per cent of the surface of Makemake, providing us with an optimal amount of data to look for any surface variation. To calculate spectral slopes, we normalized our visible spectra at 0.65 μm and fitted the 0.55–0.65 μm region with a linear function. The calculated values of the slope (mean ~9 ± 3 per cent/1000 Å) are consistent with those from the literature and show only minor variations compatible within the errors. This can suggest ether very homogenous surface of Makemake or near pole-on aspect. However, as it was discussed in [3] a nearly edge-on configuration seems to be more preferable.

In order to measure the band shifts we ran a cross-correlation analysis between our spectra and the spectral model of pure methane. We found our average value of the band shifts (−6.2 ± 1.9 Å) to be in good agreement with the previously reported blue-shift of ~−4 Å [4].

To constrain the surface composition of Makemake, we applied Shkuratov spectral model [5]. We consider both large and small methane ice particles, and found that Makemake's surface is dominated by cm-sized methane ice grains (which is rather an indicator of a long path length), while the presence of small ones is limited to a few per cent. Inclusion of tholins and methane irradiation products into our model lowers the RMSD value compared to that of pure methane ice (cf. Figure 3). But given that spectral resolution of our data is too low for direct detection of those products, our final model suggests rather a possibility of the presence of irradiation products on the surface of Makemake, not a unique solution.

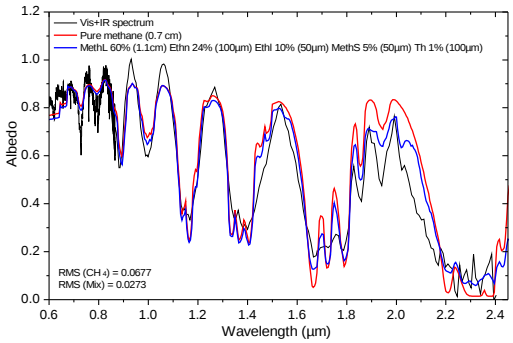

Figure 3: Spectrum of Makemake (black), fitted by a model (blue) of methane ice (Large grains: 60%; Small grains: 5%) plus ethane (24%), ethylene (10%) and Ice tholins (1%). A model of pure methane ice (red) is shown for comparison.

4. Summary and Conclusions

We present new visible and NIR spectral observations of the dwarf planet Makemake, that cover most part of the surface. The obtained spectra are dominated by methane ice absorption bands and are slightly blue-shifted, probably due to a partial dilution of methane in nitrogen. Our data suggest a very homogeneous surface, which is supported by the discovery of a Makemakean moon (to explain previously detected heterogeneities) and probable equator-on configuration. Hence, our data do not support the hypothesis of atmospheric freeze-out and escape episodes with consequent local colour changes. Spectral modelling results suggest that the surface of Makemake is dominated by large cm-sized methane ice grains (or a slab) eventually covered with a thin layer of small particles and possible presence of higher mass alkanes (such as ethane and ethylene).

References

[1] Belskaya, I., et al.: Polarimetry of trans-Neptunian objects (136472) Makemake and (90482) Orcus, A&A, Vol. 547, 101, 2012.

[2] Lim T. L. et al.: "TNOs are Cool": A survey of the trans-Neptunian region III. Thermophysical properties of 90482 Orcus and 136472 Makemake, A&A, Vol. 518, L148, 2010.

[3] Parker, A. H. et al.: Discovery of a Makemakean Moon, AJ, Vol. 825, L9, 2016.

[4] Lorenzi V., Pinilla-Alonso N., and Licandro J.: Rotationally resolved spectroscopy of dwarf planet (136472) Makemake, A&A, Vol. 577, p. 86, 2015.

[5] Shkuratov Yu., et al.: A Model of Spectral Albedo of Particulate Surfaces: Implications for Optical Properties of the Moon, Icarus, Vol. 137, 235, 1999.

EPSC Abstracts
Vol. 11, EPSC2017-448, 2017
European Planetary Science Congress 2017
© Author(s) 2017

The enigmatic colors of the Centaur population

E. Mazzotta Epifani (1), E. Dotto (1), S. Ieva (1), D. Perna (1,2), P. Palumbo (3,4), M. Micheli (1,5), E. Perozzi (6)
(1) INAF – Osservatorio Astronomico di Roma, Via Frascati 33, 00078 Monte Porzio Catone (Roma), Italy
(2) LESIA – Observatoire de Paris, 5 place J. Janssen, 92195 Meudon, France
(3) Università Parthenope, Dip. Sci. & Tecn., Centro Direzionale Isola C4, 80143 Napoli, Italy
(4) INAF – Istituto di Astrofisica e Planetologia Spaziale, Via Fosso del Cavaliere 100, 00133 Roma, Italy
(5) ESA SSA-NEO Coordination Centre, Frascati (Roma), Italy
(6) Agenzia Spaziale Italiana – ASI, Via del Politecnico snc, 00133 Roma, Italy
elena.epifani@oa-roma.inaf.it

Abstract

Centaurs are considered “transition bodies”, from the cold inactive Kuiper Belt Objects beyond Neptune to the active Jupiter Family comets. Their visual colors apparently divide the population into two distinct groups, one with grey, solar-like colors and one with redder colors. It is still unclear if this peculiar color distribution (unique in the Solar System) is due to different thermal reprocessing on their surface or to different composition and/or region of origin. The issue is further complicated by the fact that more and more Centaurs are observed with a comet-like behavior, and they all fall in the grey clump (as the few comet nuclei characterized up to now), even if very recently few active Centaurs were found with colors that classified them in between the two groups.

1. Introduction

Centaurs form a dynamical class of minor bodies in the Solar System moving on highly chaotic and unstable orbits in the region between Jupiter’s and Neptune’s orbits. With orbital lifetimes of the order of 10^6 years [1], Centaurs are brief residents in the region between the gas giant planets, and those who survive the dynamical environment in this region may become Jupiter family comets (JFCs) [2,3]. As they are considered “transition objects” from the inactive Kuiper Belt Objects to the active JFCs, the study of their physical properties is a main topic to assess the relationship and establish reliable patterns between the object classes, and to constrain the evolution of minor bodies in the Solar System.

Centaurs exhibit a physical property not observed among any other objects in the Solar System: their visual colors apparently divide the population into two distinct groups, the ”grey ones” (with neutral, solar-like colors) and the ”red ones” (with very red colors) [4]. The color properties of this class of targets are crucial to obtain reliable hints on the surface properties and their evolution within the Solar System: it is still unclear if the peculiar color distribution of Centaurs is due to different thermal reprocessing on their surface [4] or to a different composition and/or region of origin [5,6].

A few Centaurs (28 objects over a family of ∼ 300 members, i.e., around 10% of the whole sample, as per April 2017) have been observed with a well developed dust coma in optical images. The first example was (2060) Chiron, which orbits at about 10 AU from the Sun and shows a sustained, though variable, cometary-like activity along its orbit [7,8]. Very few active Centaur has been fully characterized up to now: many of them have dust loss rate Q_d comparable or even higher than several active comets at much smaller heliocentric distances [9,10,11,12]. On the other side, there are few active Centaurs that can be considered quite weak dust emitters, despite their relatively close perihelion distance, with Q_d less than ∼ 10 kg/s [9,13,14]. As a group, the main general properties of the active Centaurs was, up to very recently, that they clustered in the grey group among the whole sample, and their mean colors overlapped with those of the Jupiter Family Comets (JFC) nuclei. Only recently [15], few active Centaurs were found for the first time with colors that classified them as “intermediate” among the two groups. Actually, it is not yet possible to formally conclude at the 3σ level of confidence that the active and inactive Centaurs have different (uni-modal and bi-modal) color distributions. Figure 1 summarizes

the present state-of-the-art of the color-color distribution of the Centaur population.

The question of Centaur colors and their relationship with comet-like activity is a still open issue: one hypothesis is that the "primordial" surface of bodies coming from the Kuiper Belt, consisting of irradiated organics spread on a more or less thick surface layer, is progressively blanketed with "fresh", unirradiated material expelled from beneath after the rise of comet-like activity. Blanketing timescales are quite uncertain, since Centaur activity could be episodic and fallback will be not, in general, uniformly distributed on the nucleus surface, but some observational evidences allow to estimate that it could be very short (0.1-10 years) compared to the typical dynamical lifetime (10^6-10^7 years) of a Centaur [15]. The presence of red and ultra-red matter on the nucleus surface of active Centaurs, never observed up to now, can be considered fundamental test to constrain the "fallback blanketing hypothesis".

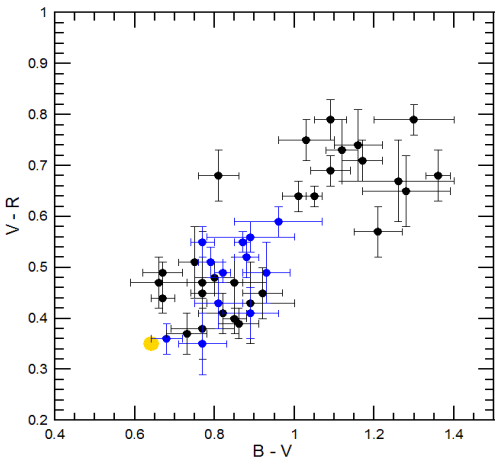

Figure 1: Color-color diagram comparing the inactive Centaurs (black dots) with the active ones (blue dots): data are taken from [9,13,15,16]. The yellow dot shows the color of the Sun.

In this talk we will present an overview of the current status and of the still open questions about the intriguing issue about the color of Centaurs, also in the more general framework of the dynamical and evolutionary link about groups of small bodies in the Solar System. We will also present the first results of an ongoing large observing program specifically tailored on the Centaurs' colors, and discuss about the investigation of the actual comet-like activity frequency in the group, which could in some case stymie the physical studies about these objects.

References

[1] Tiscareno M.S. & Malhotra R., 2003, AJ 126, 3122
[2] Levison H.F. & Duncan M.J., 1997, Icarus 127, 13
[3]Horner J. et al., 2004, MNRAS 354, 798
[4] Melita M.D. & Licandro J., 2012, A&A 539, A144
[5] Peixinho N. et al., 2012, A&A 546, A86
[6] Fraser W.C. & Brown M.E., 2012, ApJ 749, 33
[7] Luu J.X. & Jewitt D.C., 1990, AJ 100, 913
[8] Meech K.J. & Belton M.J.S., 1990, AJ 100, 1323
[9] Jewitt D.C., 2009, AJ 137, 4296
[10] Mazzotta Epifani E. et al., 2006, A&A 460, 935
[11] Mazzotta Epifani E. et al., 2011, MNRAS 415, 3097
[12] Lacerda P., 2013, MNRAS 428, 1818
[13] Mazzotta Epifani E. et al., 2014, A&A 565, A69
[14] Mazzotta Epifani E. et al., 2017, A&A 597, A59
[15] Jewitt D.C., 2015, AJ 150, 6, 201
[16] Peixinho N. et al., 2003, A&A 410, L29

EPSC Abstracts
Vol. 11, EPSC2017-645-1, 2017
European Planetary Science Congress 2017
© Author(s) 2017

Predictions of stellar occultations by Chariklo using Gaia DR1 catalog and results of 3 campaigns observed in 2017

D. Bérard (1), B. Sicardy (1), J.I.B. Camargo (3,5), J. Desmars (1), R. Leiva (2,6), F. Braga-Ribas (3,4), J. L. Ortiz (2), R. Vieira-Martins (3)
(1) LESIA, Observatoire de Paris, PSL Research University, CNRS, Sorbonne Universités, UPMC Univ. Paris 06, Univ. Paris Diderot, Sorbonne Paris Cité, France (2) Instituto de Astrofísica de Andalucía (CSIC), Granada, Spain, (3) Observatório Nacional/MCTI, Rio de Janeiro, Brazil, (4) Federal University of Technology-Paraná (UTFPR / DAFIS), Curitiba, Brazil, (5) Laboratório Interinstitucional de e-Astronomia-LINEA, Rio de Janeiro, Brazil, (6) Instituto de Astrofísica, Facultad de Física, Pontificia Universidad Católica de Chile, Santiago, Chile

Abstract

We will report the results of 3 stellar occultations by the Centaur Chariklo and its ring system observed in 2017. Those events have been predicted using Gaia catalog DR1 released on September 15, 2016, leading to accuracy better than 5 mas (50km projected at Chariklo's distance). We were able to scan deeply the main ring C1R, and put constraints on the shape and size of the main body. Improvements in the prediction method due to Gaia catalog will also be explained.

1. Introduction

Two dense and narrow rings around Chariklo (the largest centaur object known to date, diameter of 250 km) were discovered by stellar occultation on June 3, 2013 [2]. During the past 4 years, 16 other occultations by Chariklo have been observed in order to better understand and characterize Chariklo's system. The occultations observed before the end of 2016 are presented in [1] and here we present occultations observed in 2017. Rings subtend 80 mas projected in the sky so the only way to study them is by using stellar occultation method: when the body comes in front of a background star it will block the light. By studying the light curve of the star, we access information about the object and its vicinity. Until September 2016, the accuracy of the predictions did not allow to study globally the ring structure and the shape of Chariklo's main body. Gaia catalog DR1 changes the spirit of the prediction by achieving accuracy of a few milli-arcseconds (mas).

2. Predictions based on Gaia DR1

Gaia DR1 contains the astrometry of one billion stars (with no proper motions). It allows us to improve the accuracy of a prediction by a factor of at least 5. We also compared several methods to obtain a correct proper motion (UCAC5, TGAS, UCAC4-DR1). Then we reduce our previous occultations and astrometric observations of Chariklo using DR1. Those data were used to feed NIMA (Numerical Integration of the Motion of an Asteroid, see [3]). Fig. 1 and 2 show the Observed-Calculated of Chariklo's orbit after this improvement. One will note that the error bars (gray area) are now less than 10 mas. Combining an excellent star position and good object ephemeris leads to predictions better than 5 mas in RA and DEC.

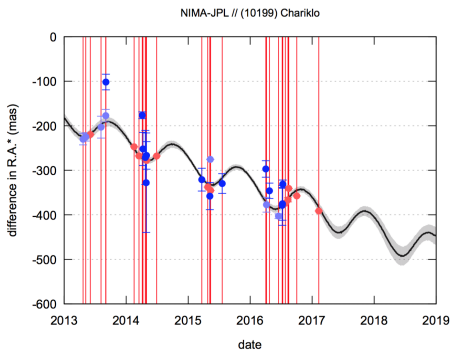

Figure 1: Difference in RA between last version of NIMA and JPL ephemerides. Red dots are occultations positions. Blue dots are CCD observations. Gray area represents the uncertainty of the NIMA ephemeris.

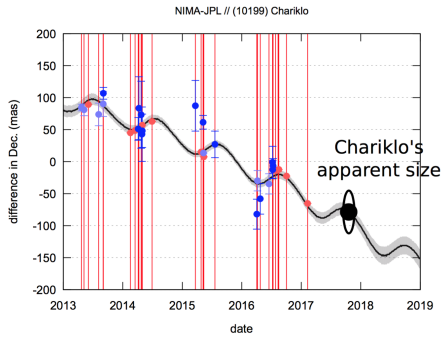

Figure 2: Same than Fig 1 for DEC. Chariklo's apparent size has been added for comparison.

3. The three occultations observed in 2017

Three very favorable occultations by Chariklo are predicted for 2017: on April 9, and June 22 from Namibia and on July 23 from South America (predicted maps are presented respectively in Fig. 3, 4, 5). Good results have already been obtained on April 9 and will be presented. And if positive, results of June 22 and July 23 events will also be given.

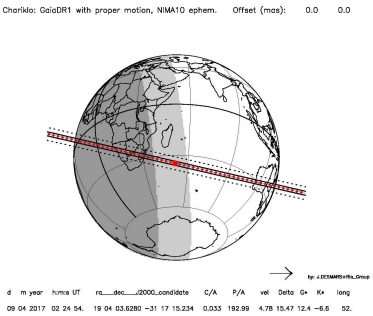

Figure 3: Prediction map of the April 9, 2017 event. Red dots are spaced by 1 min. Solid lines represent main body shadow limits, whereas dotted lines represent rings shadow boundaries. Nominal time of the occultation given under the plot corresponds to the time of closest approach, drawn as the biggest red dot. The arrow (bottom right) indicates the direction of the shadow motion.

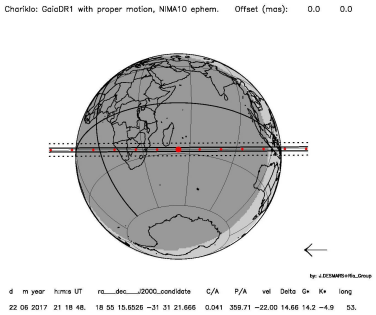

Figure 4: Same than Fig 3 for the June 22, 2017 event.

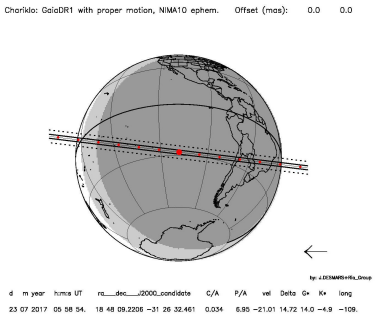

Figure 5: Same than Fig 3 for the July 23, 2017 event.

Acknowledgements

Part of the research leading to these results has received funding from the European Research Council under the European Community's H2020 (2014-2020/ ERC Grant Agreement n 669416 LUCKY STAR).

References

[1] Bérard, D.; Sicardy, B.; Braga-Ribas F.; Camargo, J; Desmars, J.; Ortiz,J-L. ; Meza, E.; Vieira-Martins, R.;Duffard, R.; Assafin, M.; Kervella, P.; Leiva Espinoza, R.; Richichi, A.; Puji, I.; Colas, F.; Lecacheux, J.; De Witt, C.; Breytenbach, H.; Sickafoose, A.; Dauvergne. J-L.; Schoenau, P.;Bath, K-L.; Beisker, W.; Maquet, L.; Bradshaw, J.; Tancredi, G.; Roland, S.; Salvo, R.; Selman, F.; Herrera, C.; Carraro, G.,; Brillant, S.; Dumas, C.; Ivanov, V.; Maury, A.; Colazo, C.; Pollock, J.; Jehin, E.; Monaco, L.; Prager, R.; Bilios, S.; Nardon, J.; Melia, R.; Spagnotto, J.; Blain, A.; Broughton, J.; Cool, A.; Lade, B.; Kerr, S.; Vachier, F.; Teng, J-P.; Pavlov, H.; Bode, H.; Herald, D.; Loader, B.; Hill, K.; Gault, D.; Newman, J.; Barry, T., 2017, Structure of Chariklo?s ring system, Submitted to Astronomical Journal

[2] Braga-Ribas, F., Sicardy, B., Ortiz, J.L., Snodgrass, C., Roques, F., Vieira-Martins, R., Camargo, J.I.B., Assafin, M., Duffard, R., Jehin, E., Pollock, J., Leiva, R., Emilio, M., Machado, D.I., Colazo, C., Lellouch, E., Skottfelt, J., Gillon, M., Ligier, N., Maquet, L., Benedetti-Rossi, G., Gomes, A.R., Kervella, P., Monteiro, H., Sfair, R., El Moutamid, M., Tancredi, G., Spagnotto, J., Maury, A., Morales, N., Gil- Hutton, R., Roland, S., Ceretta, A., Gu, S.H., Wang, X.B., Harpsoe, K., Rabus, M., Manfroid, J., Opitom, C., Vanzi, L., Mehret, L., Lorenzini, L., Schneiter, E.M., Melia, R., Lecacheux, J., Colas, F., Vachier, F., Widemann, T., Almenares, L., Sandness, R.G., Char, F., Perez, V., Lemos, P., Martinez, N., Jorgensen, U.G., Dominik, M., Roig, F., Reichart, D.E., Lacluyze, A.P., Haislip, J.B., Ivarsen, K.M., Moore, J.P., Frank, N.R., Lambas, D.G., 2014. A ring system detected around the Centaur (10199) Chariklo. Nature 508, 72?75.

[3] Desmars, J., Camargo, J.I.B., Braga-Ribas, F., Vieira-Martins, R., Assafin, M., Vachier, F., Colas, F., Ortiz, J.L., Duffard, R., Morales, N., Sicardy, B., Gomes-Júnior, A.R., Benedetti-Rossi, G., 2015. Orbit determination of trans-Neptunian objects and Centaurs for the prediction of stellar occultations. Astron. Astrophys. 584, A96.

EPSC Abstracts
Vol. 11, EPSC2017-721, 2017
European Planetary Science Congress 2017
© Author(s) 2017

Thermal emission of the Eris-Dysnomia system

Cs. Kiss (1), T.G. Müller (2), E. Lellouch (3), E. Vilenus (4) and Á. Kóspál (1)
(1) Konkoly Observatory, MTA CSFK, Hungary (2) Max-Planck-Institut für extraterrestrische Physik, Garching, Germany
(3) LESIA, Observatoire de Paris, Meudon, France (4) Max-Planck-Institut für Sonnensystemforschung, Göttingen, Germany

Abstract

We present a thorough analysis of the far-infrared and submillimeter emission of the Eris-Dysnomia dwarf planet system. The systems shows a clear flux density excess at the shortest far-infrared wavelengths (70-100 μm) indicating the presence of the warm component in the thermal emission, in addition to the very cold (<30K) Eridian surface. We discuss several scenarios that could explain this excess emission.

1. Introduction

Eris is the 2nd largest dwarf planet known in the Solar system, with a size very similar to Pluto, and at the same time the most massive one. Its mass is known from the orbit of its moon, Dysnomia. The largest dwarf planets typically have very high (>50%) geometric albedos, and usually the same bright surface is assumed for the typically faint moons around them (see e.g. the Haumea system). While visible range photometric observations provide little information of the size and surface properties of these bodies, their thermal emission is an exteremly useful tool in unraveling their basic physical characteristics.

2. Observations

The Eris-Dysnomia system was observed with the PACS photometer of the Herschel Space Observatory at several epochs in the 70, 100 and 160 μmm bands in the framework of the TNOs are Cool! Open Time Key Program (Müller et al., 2009), as well as in dedicated Open Time Programs (PI: E. Vilenius). The latter observations are among the deepest ones ever taken with PACS photometer at 160 μm. Spitzer/MIPS 24 and 70 μm measurements were also taken at earlier epochs. Additional observations were performed with the ALMA millimeter array telescope system (PI: M. Brown), and resulted in a successful detection of Eris at three epochs, providing a strong constraint on the 873 μm flux.

3. Results

The analysis of the combined SED clearly shows that the observed thermal emission cannot be explained with a single, cold, high albedo terrain that is otherwise suggested by e.g. the occultation observations. An additional, warm (>40K) component is needed that in principle may be (1) dark terrain with suitable geometry configuration on the surface of Eris, (2) a large (D>500 km) and low albedo (pV<5%) Dysnomia, (3) hot (50 K) regions on the Eridian surface powered by cryovolcanic activity, (4) an extended ring of dark dust particles or (5) long-wavelength emissivity changes. We are giving a detailed comparison of these possibilities and evaluate the probabilities in the light of the current observations.

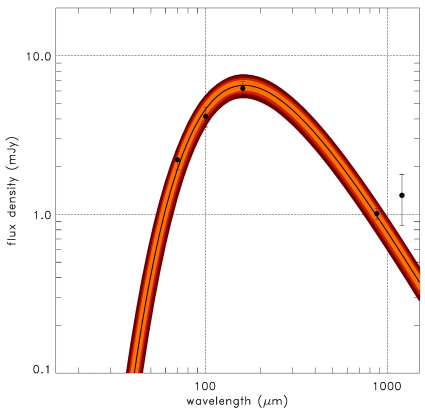

Figure 1: Spectral enegry distribution of the thermal emission of Eris. While the observed fluxes can be well fitted with a single terrain model (as shown in this figure) the corresponding size does not agree with the occultation results.

Acknowledgements

The research leading to these results has received funding from the European Union's Horizon 2020 Research and Innovation Programme, under Grant Agreement no 687378.

EPSC Abstracts
Vol. 11, EPSC2017-793, 2017
European Planetary Science Congress 2017
© Author(s) 2017

Chaotic scattering of main belt asteroids from Centaurs and Trans-Neptunian Objects

M. A. Galiazzo (1,2), P. Wiegert (2), S. Aljbaae (3)

(1) University of Vienna, Vienna, Austria, (2) The University of Western Ontario, Canada Università di Padova, Italy, (3) Universidade Estadual Paulista, Brazil (mattia.galiazzo@univie.ac.at – mattia.galiazzo@gmail.com)

Abstract

Centaurs are objects whose orbits are found between those of the giant planets. They are supposed to originate mainly from the Trans-Neptunian objects, and they are among the sources of Near-Earth Objects (TNOs). We investigate their interactions with main belt asteroids to determine if chaotic scattering caused by close encounters and impacts by these bodies may have played a role in the dynamical evolution of the main belt. We find that Centaurs and TNOs (C+TNOs) that reach the inner Solar System can modify the orbits of main belt asteroids, though only if their mass is of the order of 10^{-9} $m_{\odot}$ for single encounters or, one order less in case of multiple close encounters. Current main belt asteroids that originated as C+TNOs may lie in the outer belt, most likely between 2.8 au and 3.2 au (though at larger eccentricities than typical of main belt asteroids) but also in its outer regions.

1. Introduction

Centaurs are objects whose orbits are contained between those of Jupiter and Neptune (Bayley et al. 2009). Currently[1] 301 Centaurs are known (JPL Small-Body Database Search Engine at http://ssd.jpl.nasa.gov/sbdb query.cgi) and the population of objects with diameters larger than 1 km is estimated to be more then ∼ 40 thousand (Horner, Evans & Bailey 2004a). Since Centaurs and their progenitors can be relatively massive (∼ lunar mass), move throughout the planetary system, and have done so throughout its existence and in much larger numbers in the past, we ponder whether close encounters and impacts by Centaurs on main belt asteroids may have played a role in the dynamical evolution of the have played a role in the recent (that is, after theLate Heavy Bombardment, from 3.8 Gyrs ago to now) dynamical evolution of the main belt and particularly asteroid families.

1 June 2015

2. Methods

We consider two time spans: (i) the present population (PP), reaching 50 Myr into the past, examines the effect of Centaurs and TNOs encounters on young asteroid families, i.e. the Karin family (5.3 Myr, Nesvorny et al. 2002). (ii) The ancient population, AP, stretches back 3.8 Gyrs ago (Hartmann et al. 2000; Kirchoff et al. 2013), the estimated age of the end of the Late Heavy Bombardment (LHB) process, and examines the effects on old asteroid families, e.g. Flora family, which is old ∼4.4 Gyr (Carruba et al. 2016). In particular, we investigate the close encounters with Centaurs and TNOs (from now on C+TNOs), with a diameter larger than 100 km, can perturbate/diffuse young and/or old main belt families (Zappala et al. 1995; Migliorini et al. 1995; Nesvorny 2012; Novakovi c et al. 2011). An example is the scattering of V-type (basaltic) asteroids from the Vesta family beyond the 3J:1 mean motion resonance,into the central and outer main belt, see also Carruba et al. (2014); Huaman et al. (2014). We also consider whether Centaurs contribute to the presence of interlopers inside families, like the case of the C-types (carbonaceous asteroids) in the Hungaria family (up to 6%, Warner et al. 2009), whose member are in majority E-types. In order to do this, we use the Lie-numerical integrator set to precision 10-13 (Hanslmeier and Dvorak 1984, Eggl and Dvorak 2010; Bancelin et al. 2012, Galiazzo et al. 2013a; Galiazzo and Schwarz 2014).

3. Results and conclusions

The most perturbed regions of the belt are shown in the lower panel of Fig. 1 (Galiazzo, Wiegert &

Aljbaae, 2016), which illustrates the perturbed region of the AP by a line connecting aphelion and perihelion. The most influenced region is the Outer main belt at low inclinations. Fig. 2 show a drift of a C+TNO in the main belt region.

Some C+TNOs stay for relatively long periods in the main belt in our simulations, up to 3 Myrs (3.7 Myrs for the AP case), with some low-
eccentricity orbits, e ∼ 0.1.

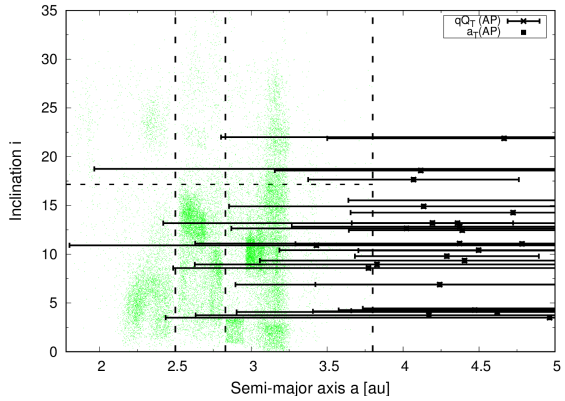

Figure 1: The semi-major axis of the main belt asteroids with H < 14 is represented with small green dots. The larger black points represent the C+TNO populations when they first enter the main-belt: their semi
-major axis (aT with aphelion and perihelion limits) versus
inclination projection of the TNOs of the Ancient Population.

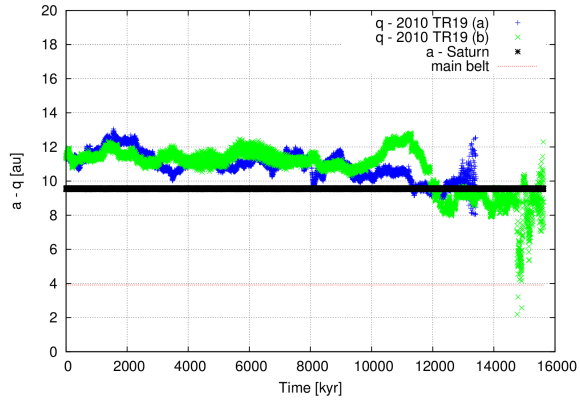

Figure 2: Drift in the main belt of 2 clones of the asteroid 2010 TR19.

Acknowledgements

MAG wants to acknowledgevthe support by the Austrian FWF project P23810-N16 and the “Reitoria de pos-gradua¸cao da UNESP” (PROPg, grant PVExt-2015). The core part of this work was done when MAG has been present at UNESP as ”visiting fellow”. MAG wants also to thanks Prof. V. Carruba for his important suggestions for the paper and Dr. Y. Cavecchi for suggestions in computational improvements and Prof. A. Morbidelli for data on the population decay of the TNOs. SA wants to thank Brazilian National Research Council (CNPq, grant 13/15357-1). This work was also supported in part by the Natural Sciences and Engineering Research Council of Canada.

References

[1] Bailey, B.L. and Malhotra, R.: Icarus 203, 155, 2009.

[2] Bancelin, D., Hestroffer, D. and Thuillot, W.: Celestial Mechanics and Dynamical Astronomy 112, 221, 2012

[3] Carruba, V., Nesvorny, D., Aljbaae, S., Domingos, R.C. and Huaman, M.: Mon. Not. R. Astron. Soc. 458, 3731, 2016.

[4] Eggl, S. and Dvorak, R.: In: Souchay, J., Dvorak, R. (eds.), Lecture Notes in Physics, Berlin Springer Verlag, 790, 431, 2010.

[5] Galiazzo, M.A., Bazso, A. and Dvorak, R.: Planet. Space Sci., 84, 5, 2013.

[6] Galiazzo, M.A. and Schwarz, R.: Mon. Not. R. Astron. Soc., 445, 3999, 2014.

[7] Hanslmeier, A. and Dvorak, R.: Astron. Astrophys. 132, 203, 1984.

[8] Hartmann, W.K., Ryder, G., Dones, L. and Grinspoon, D.: Canup, R.M., Righter, K., et al.(eds.) The Time Dependent Intense Bombardment of the Primordial Earth/Moon System, p. 493, 2000.

[9] Horner, J., Evans, N.W. and Bailey, M.E.: Mon. Not. R. Astron. Soc. 354, 798, 2004a.

[10] Huaman, M.E., Carruba and V., Domingos, R.C.: Mon. Not. R. Astron. Soc., 444, 2985, 2014.

[11] Kirchoff, M.R., Chapman, C.R., Marchi, S., Curtis, K.M., Enke, B. and Bottke, W.F.: Icarus 225, 325, 2013.

[12] Migliorini, F., Zappala, V., Vio, R. and Cellino, A.: Icarus 118, 271, 1995.

[13] Nesvorny, D., Bottke, W.F. Jr., Dones, L. and Levison, H.F.: Nature 417, 720, 2002.

[14] Nesvorny, D.: NASA Planetary Data System 189, 2012.

[15] Novakovic, B., Cellino, A., Knezevic, Z.: Icarus 216, 69, 2011.

[16] Zappala, V., Bendjoya, P., Cellino, A., Farinella, P. and Froeschle, C.: Icarus 116, 291, 1995.

EPSC Abstracts
Vol. 11, EPSC2017-804, 2017
European Planetary Science Congress 2017
© Author(s) 2017

Pluto's Atmospheric Haze

A. F. Cheng[1], M. E. Summers[2], G. R. Gladstone[3], D. F. Strobel[4], L. A. Young[5], P. Lavvas[6], J. A. Kammer[5], C. M. Lisse[1], A. H. Parker[5], E. F. Young[5], S. A. Stern[5], H. A. Weaver[1], C. B. Olkin[5], K. Ennico[7]

(1) The Johns Hopkins University Applied Physics Laboratory, Johns Hopkins Road, Laurel, MD, USA (andrew.cheng@jhuapl.edu / 01 240 228-5415)
(2) George Mason University, Fairfax, VA, USA
(3) Southwest Research Institute, San Antonio, TX, USA
(4) The Johns Hopkins University, Baltimore, MD, USA
(5) Southwest Research Institute, Boulder, CO, USA
(6) University of Reims, Reims, France
(7) NASA Ames Research Center, Moffett Field, CA, USA

Abstract

Haze in Pluto's atmosphere was detected by New Horizons approach and departure imaging and by the UV solar occultation experiments. Layered haze was detected from the surface up to altitudes above 200 km in the visible at solar phase angles from ~20° to ~169°, and it was detected up to 300 km altitude in the UV occultation. The haze is strongly forward scattering in the visible, and a microphysical model of haze reproduces the visible phase function just above the surface with 0.5 µm spherical particles, but also invokes fractal aggregate particles to fit the visible phase function at 45 km altitude and to account for UV extinction. The visible phase function at the bottom of the atmosphere has a back scatter lobe which is absent from the phase function measured 45 km above the surface, making the latter phase function similar to that for haze in Titan's upper atmosphere. Pluto's haze may form by similar processes to those responsible for the detached haze layer in the upper atmosphere of Titan. It is suggested that haze particles form fractal aggregates which grow larger and more spherical as they settle downwards through the bottom 15 km of the atmosphere. Haze particles settle onto Pluto's surface, at a rate sufficient to alter surface optical properties on seasonal (hundred-year) time scales. However, if this picture applies to Pluto's atmosphere throughout the Pluto year, then haze particles would rapidly accumulate to an optically thick surface layer within thousands of years. If the compositions of deposited haze particles are regionally uniform across Pluto, the striking albedo and color contrasts on Pluto, with very bright and dark regions, would be difficult to understand. Pluto's regional scale albedo contrasts may be preserved by atmospheric collapse [1].

Acknowledgements

We gratefully acknowledge support from NASA under the New Horizons project.

References

[1] Cheng A. F. et al. (2017) Haze in Pluto's Atmosphere. Icarus, 290: 112-133.

EPSC Abstracts
Vol. 11, EPSC2017-856, 2017
European Planetary Science Congress 2017
© Author(s) 2017

Hyper Suprime-Cam Lightcurve Studies of Trans-Neptunian Objects from the Outer Solar System Origins Survey

M. Alexandersen (1), S. Benecchi (2), Y-T. Chen (1), M. E. Schwamb (3), S-Y. Wang (1), M. Lehner (1), P. Lacerda (4), A. Thirouin (5), N. Peixinho (6)

(1) Academia Sinica Institute of Astronomy and Astrophysics, 11F of AS/NTU Astronomy-Mathematics Building, No. 1, Sec. 4, Roosevelt Rd., Taipei 10617, Taiwan, R.O.C. (2) Planetary Science Institute, 1700 East Fort Lowell, Suite 106, Tucson, AZ 85719, USA (3) Gemini Observatory, Northern Operations Center, 670 N. A'ohoku Place, Hilo, Hawaii, 96720, USA (4) Queen's University Belfast, University Road, Belfast, BT7 1NN, Northern Ireland, UK (5) Lowell Observatory, 1400 W. Mars Hill Rd, Flagstaff, AZ 86001, USA (6) Unidad de Astronomía, Fac. de Ciencias Básicas, Universidad de Antofagasta, Avda. U. de Antofagasta 02800 Antofagasta, Chile (mike.alexandersen@alumni.ubc.ca)

Abstract

Lightcurves can reveal information about the gravitational and/or collisional processes that have acted on small bodies since their formation. High quality lightcurves provide constraints on the material properties and interior structure of individual objects. In large samples, lightcurves can shed light on the formation source of small body populations. We have studied 71 TNOs from the Outer Solar System Origins Survey (OSSOS) using Hyper Suprime-Cam (HSC) on the 8.2-m Subaru Telescope, in a one-night study of 15 OSSOS TNOs in 2014 and a two-night lightcurve study of 65 OSSOS TNOs in 2016, with nine objects overlapping between the two studies. Subaru's large aperture and HSC's large field of view enables measurements of multiple TNOs with a range of magnitudes ($m_r = 22.5$ to 25.1) in each telescope pointing. The OSSOS objects span from several hundred kilometres to a few tens of kilometres in diameter, and have well-determined orbits and dynamical classifications. Our sample thus enables examining the variability in different dynamical sub-classifications (such as the cold classicals and hot populations) for smaller objects than previous lightcurve projects have typically studied.

1. OSSOS

OSSOS [1] is a large, well-characterised TNO survey on the Canada-France-Hawaii Telescope (CFHT), having surveyed 160 sq.deg. of sky, detecting over 900 TNOs down to $m_r \approx 25.1$. All detected objects are tracked to ensure well-determined orbits, allowing securely classified among the various TNO sub-populations (resonant, classical, scattering, etc.). We choose to observe TNOs from OSSOS because they are recently discovered (allowing multiple objects per field due to high on-sky density) and their well-determined orbits allows us to compare populations. Previous light curve studies have been reported for ~ 90 TNOs [5, 3, 2], but that sample has unknown selection biases and discovery circumstances. By targeting OSSOS TNOs, our discovery and selection biases are well understood and can be accounted for.

2. Data and methodology

All data was taken using HSC on Subaru Telescope. One night in 2014 obtained 300 second exposures of two fields (containing 12 and 7 TNOs) at 12 times over the course of 6 hours. In August 2016 we targeted six fields, observing each with a 300 second exposure time before repeating the fields, for a measurement separation of just over half an hour and SNR of about 60 for an $m_r = 23.8$ object. Two field were observed a total of 20 times while four fields were observed 24 times over two nights.

Our photometric measurements were done using the TRIPPy python package [4], thus correcting for the slight TNO movement during the exposure (movement is less than PSF FWHM) by using an elongated aperture. The photometry was subsequently calibrated relative to non-variable field stars to remove non-TNO related variability (such as weather). We use a Phase Disperion Minimization (PDM) code to estimate periods for the light curves, as described in [2]. This solution is usually degenerate, as light curves can be single peaked (albedo dominated) or double peaked (shape dominated), and aliasing is a problem, where some periods cannot be ruled out due to the timing of the observations.

3. Results

The Figure 1 histograms show that our sample spans a range of semi-major axis and absolute magnitude, H_r (CFHT r). Also plotted are histograms of the standard deviation and estimated amplitude of the light curve variation. Figure 2 shows a few examples of light curves from our sample. We will present our findings from comparing the light curve properties (period, amplitude) to orbital properties (dynamical class, orbital elements).

4. Summary and Conclusions

We have obtained one to three nights of light curve observations of 71 TNOs using HSC on Subaru Telescope. The large aperture and field of view observed up to 12 objects at once, with magnitudes from $m_r = 22.5$ to 25.1. The light curves have been photometrically calibrated and light curve periods and amplitudes have been estimated. A full analysis of correlations between light curve properties and orbital properties will be presented at EPSC.

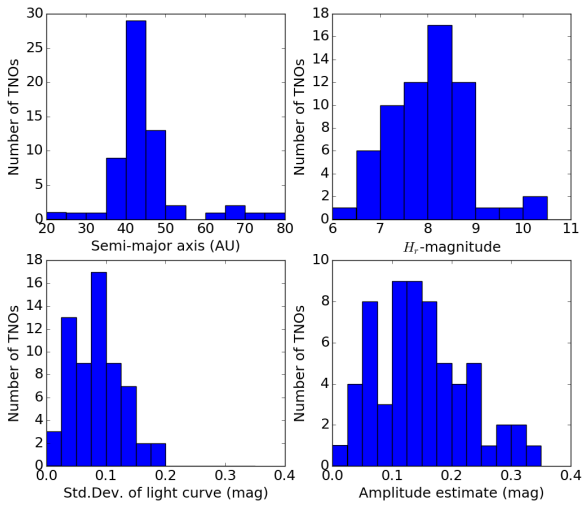

Figure 1: Histograms of semi-major axis, absolute magnitude, light curve standard deviation and estimated light curve amplitude for our HSC sample. In order to minimise spurious results caused by noise, the standard deviation and estimated amplitude are calculated ignoring the highest and lowest point in our data.

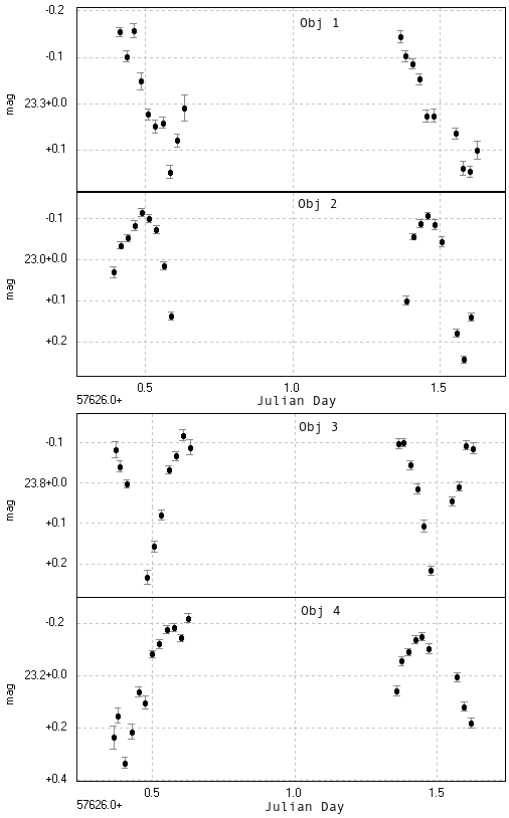

Figure 2: Light curves of four clearly variable objects from our 2016 HSC data.

References

[1] Bannister, M. T., and 38 colleagues 2016. The Outer Solar System Origins Survey. I. Design and First-quarter Discoveries. The Astronomical Journal 152, 70.

[2] Benecchi, S. D., Sheppard, S. S. 2013. Light Curves of 32 Large Transneptunian Objects. The Astronomical Journal 145, 124.

[3] Duffard, R., Ortiz, J. L., Thirouin, A., Santos-Sanz, P., Morales, N. 2009. Transneptunian objects and Centaurs from light curves. Astronomy and Astrophysics 505, 1283-1295.

[4] Fraser, W., Alexandersen, M., Schwamb, M. E., Marsset, M., Pike, R. E., Kavelaars, J. J., Bannister, M. T., Benecchi, S., Delsanti, A. 2016. TRIPPy: Trailed Image Photometry in Python. The Astronomical Journal 151, 158.

[5] Sheppard, S. S., Lacerda, P., Ortiz, J. L. 2008. Photometric Lightcurves of Transneptunian Objects and Centaurs: Rotations, Shapes, and Densities. The Solar System Beyond Neptune 129-142.

EPSC Abstracts
Vol. 11, EPSC2017-963, 2017
European Planetary Science Congress 2017
© Author(s) 2017

LUCY: SURVEYING THE DIVERSITY OF TROJANS

H. Levison (1), C. Olkin (1) K. Noll (2), S. Marchi (1) and the *Lucy* Team
(1) SwRI Boulder, Colorado, USA, (2) NASA GSFC, Maryland, USA (hal@boulder.swri.edu)

Abstract

The *Lucy* mission, selected as part of NASA's Discovery Program, is the first reconnaissance of the Jupiter Trojans, objects that hold vital clues to deciphering the history of the Solar System. Due to an unusual and fortuitous orbital configuration, *Lucy*, will perform a comprehensive investigation that visits six of these primitive bodies, covering both the L4 and L5 swarms, all the known taxonomic types, the largest remnant of a catastrophic collision, and a nearly equal mass binary. It will use a suite of high-heritage remote sensing instruments to map geologic, surface color and composition, thermal and other physical properties of its targets at close range. *Lucy*, like the human fossil for which it is named, will revolutionize the understanding of our origins.

1. *Lucy's* Comprehensive Tour

Lucy will perform flybys of six Trojans (Tab. 1, Fig. 1) that span the diversity of the Trojan population: (3548) Eurybates, (15094) Polymele, (11351) Leucus, (21900) Orus and the (617) Patroclus-Menoetius binary. *Lucy* will also encounter the Main Belt asteroid (52246) Donaldjohanson. It will launch in 2021 and will have encounters from 2027-2033 (Tab. 2). *Lucy* leverages multiple successful missions: 1. The scientific payload traces heritage to instruments flown on New Horizons, OSIRIS-REx, and Mars Global Surveyor /Mars Expedition Rover, 2. The spacecraft has high heritage from multiple previous missions, 3. The *Lucy* team includes experienced spacecraft (Lockheed Martin), mission (GSFC), and science (SwRI) Operations Teams.

Through its unique tour, *Lucy* will provide crucial input to four of the ten Priority Questions for Planetary Science as expressed by the 2013-2022 Decadal Survey [1] (DS13):

• What were the initial stages, conditions and processes of Solar System formation?
• How did the giant planets accrete, and is there evidence that they migrated to new orbital positions?
• What governed the accretion, and what roles did bombardment by large projectiles play?
• What were the sources of primordial organic matter?

The Trojan swarms contain a wide variety of small bodies, C-, D-, and P-spectral types. Giant planet migration models indicate that they formed throughout the outer Solar System and were captured in the aftermath of migration [2]. Therefore, it is only by sampling their diversity, as *Lucy* does, that their true scientific potential can be realized.

Lucy's primary science objectives are:

1. Surface composition. *Lucy* will map the color, composition and regolith properties of the surface and determine the distribution of minerals, ices and organic species,

2. Surface geology. *Lucy* will map albedo, shape, crater spatial and size distributions, determine the nature of crustal structure and layering, and determine the relative ages of surface units,

3. Interior and bulk properties. *Lucy* will determine the masses and densities, and study subsurface composition via crater windows, fractures, ejecta blankets, and exposed bedding,

4. Satellite and ring search. *Lucy* will determine the number, size-frequency distribution and location of km-scale satellites and dense rings.

2. Figures

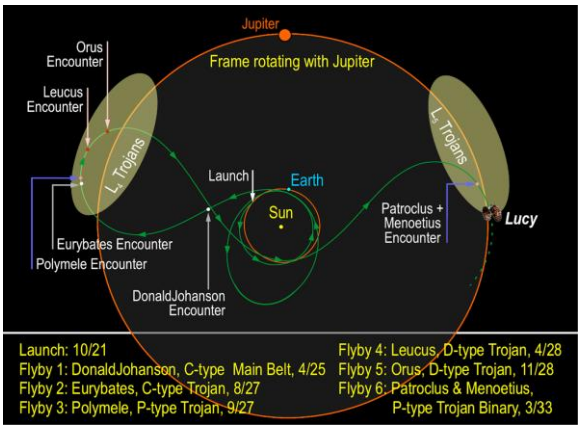

Figure 1: The trajectory of the *Lucy* mission (green) is shown in a frame fixed relative to Jupiter. Dates (month/year) for launch and encounters are noted.

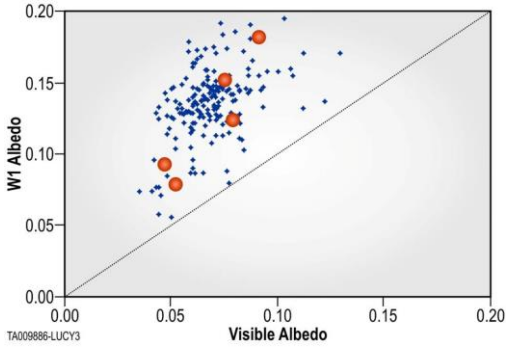

Figure 2: 540 nm and 3.4 μm albedos of the *Lucy* targets (red) are shown with all other Trojans (blue). *Lucy* targets sample the full space of Trojan albedos.

3. Tables

Table 1: Targets

Target	Diameter (km, *est.*)	Spectral Class	P_{rot} (hr)
Donaldjohanson	3.9	C	-
Eurybates	64.	C	8.7
Polymele	21.	P	6.1
Leucus	34.	D	440
Orus	51.	D	13.5
Menoetius	104.	P	103
Patroclus	113.	P	103

Table 2: Encounter circumstances.

Target	Encounter Date	Velocity (km/s)	Phase Angle*
Donaldjohanson	04/20/25	13.4	15°
Eurybates	08/12/27	5.8	81°
Polymele	09/15/27	6.0	82°
Leucus	08/18/28	5.9	104°
Orus	11/11/28	7.1	126°
Menoetius	03/02/33	8.8	56°
Patroclus	03/02/33	8.8	56°

*Approach

4. Summary

Because of their unique location near Jupiter and the critical role they play in revealing and constraining models of the formation and evolution of the Solar System, Trojans have been a high priority for space missions for over a decade. This is evidenced by calls for their reconnaissance by spacecraft in DS13 and the 2014 NASA Science Plan. Both documents identify a survey of the diversity of Trojan asteroids as one of the highest priority missions to small bodies. *Lucy* will accomplish the related goals of DS13 and the NASA Science Plan with a high-heritage, low- risk spacecraft and science payload.

References

[1] Visions and Voyages for Planetary Science in the Decade 2013-2022. National Research Council, National Academies Press (2011).

[2] Levison, H. F., et al.: Origin of the structure of the Kuiper belt during a dynamical instability in the orbits of Uranus and Neptune, Icarus, Vol. 196, pp. 258-273, 2008.

EPSC Abstracts
Vol. 11, EPSC2017-964, 2017
European Planetary Science Congress 2017
© Author(s) 2017

Dust in the Outer Solar System as measured by Cassini-CDA: KBOs, Centaurs and TNOs as parent bodies?

N. Altobelli (1), S. Kempf (2), R. Srama (3)
(1) ESA/ESAC, Madrid, Spain (2) LASP, University of Boulder, USA, (3) University of Stuttgart, Germany,
nicolas.altobelli@sciops.esa.int

Introduction

We analyse 13 years of data acquired by the Cosmic Dust Analyser (CDA)-Entrance Grid (EG) subsystem on-board the Cassini spacecraft around Saturn. We confirm the presence of exogenous dust, originating from the interplanetary space and permanently crossing the Saturnian system. We analyse the range of possible heliocentric orbital elements in order to identify their possible origin. We observe particles whose dynamics is compatible with 'old' collisional debris from the Kuiper-Belt, migrating inward the Solar System under influence of the Poynting-Robertson drag, or relatively fresh grains from recently discovered cometary activity of Centaurs. A population of particles entering the Saturn's system with high velocities can be linked to Halley-type comets as parent bodies.

1. Data analysis

The major difficulty we are facing is the identification of comparatively very rare exogenous particles in an environment dominated by E ring particles. In the densest regions of the E ring, the CDA instrument is saturated by E ring impactors, therefore 'masking' contributions from other sources. Fortunately, the Cassini spacecraft has been flying on orbits for a wide range of inclinations and eccentricities while touring Saturn during the past seven years such that regions with reduced E ring contribution can be exploited for our study. Regions more favorable for the search of exogenous particles are typically as far as possible from Saturn, or, 'far enough' from the equatorial plane of Saturn, in order to avoid the bulk of the E ring particles, as well as regions were the plasma density saturates the EG subsystem. When EG data could be acquired, the particles orbital elements can be constrained to sufficient accuracy to inambiguously discriminate E ring particles from interplanetary dust particles (IDPs).

2. Results and Discussion

The orbital elements of the IDPs are plotted on Fig. 1. The presence of IDP raining onto the Saturn's system is by itself an important result providing constraints on evolutionnary processes like, for example, the compositional evolution of atmosphere-less icy surfaces (icy moons and Saturn's main ring system) and of the atmospheres of Titan and Saturn. As importantly, from its vantage point at Saturn, about 10 AU from the Sun, the CASSINI-CDA data cast light on the dust populations of the outer solar system, their parent bodies and generation process.

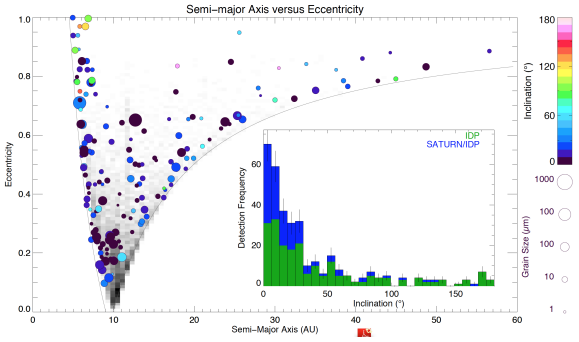

Figure 1: Orbital elements of the exogenous particles. The circles represent the heliocentric orbital elements of all exogenous solutions in an eccentricity versus semi-major axis plot. The symbol color indicates the inclination of the IDP orbits with respect to the ecliptic and the symbol size scales with the particle radius. The inset shows the corresponding inclination distribution.

We find that Jupiter Family Comets (JFCs) cannot be a dominant source for the dust that CDA measures

at Saturn. In turn, our measurements appear in good qualitative and quantitative agreement with the dynamical signature of KBO dust expected at Saturn. We find, however, that KBO dust cannot be distinguished at Saturn dynamically from particles released by Centaurs/TNOs, whose cometary-like activity at large heliocentric distances has been recently discovered. Grains released by Halley types comets, with high-heliocentric inclinations, or even of interstellar origin (distinct from the interstellar dust flow observed by Ulysses, Galileo and Stardust) are reported.